CHALMERS

An Analytical Model of a Tire's Interaction on Snow

Master's thesis in Automotive Engineering

NIKHIL BALIGA
GOKUL GOUDA HIREGOUDAR

Department of Mechanics and Maritime Sciences
CHALMERS UNIVERSITY OF TECHNOLOGY
Göteborg, Sweden 2018

MASTER'S THESIS IN AUTOMOTIVE ENGINEERING

An Analytical Model of a Tire's Interaction on Snow

NIKHIL BALIGA
GOKUL GOUDA HIREGOUDAR

Department of Mechanics and Maritime Sciences
Division of Vehicle Engineering and Autonomous Systems
Vehicle Dynamics Group
CHALMERS UNIVERSITY OF TECHNOLOGY

Göteborg, Sweden 2018

An Analytical Model of a Tire's Interaction on Snow
NIKHIL BALIGA
GOKUL GOUDA HIREGOUDAR

SUPERVISOR: FREDRIK BRUZELIUS
EXAMINER: BENGT J H JACOBSON

Master's thesis 2018:16
Department of Mechanics and Maritime Sciences
Division of Vehicle Engineering and Autonomous Systems
Vehicle Dynamics Group
Chalmers University of Technology
SE-412 96 Göteborg
Sweden
Telephone: +46 (0)31-772 1000

Cover:
graphic design showing a tire and a snowflake

Chalmers Reproservice
Göteborg, Sweden 2018

An Analytical Model of a Tire's Interaction on Snow
Master's thesis in Automotive Engineering
NIKHIL BALIGA
GOKUL GOUDA HIREGOUDAR
Department of Mechanics and Maritime Sciences
Division of Vehicle Engineering and Autonomous Systems
Vehicle Dynamics Group
Chalmers University of Technology

Abstract

Snow covered roads are a common problem during the winter months in the Northern Hemisphere. The roads become slippery due to the accumulation of snow on the surfaces and hence significantly changes the coefficient of friction, resulting in accidents. It is with this motivation the traction of a tire needs to be maximized. Unlike a tire on an asphalt surface, the tire is subjected to a complex interaction on snow. Various phenomena that contribute to the force generation on a snow surface are studied with a physical motivation in this report. By understanding the net force generation of a tire, a physical approach is used to develop a vehicle dynamics model that can be used for e.g handling simulations.

The plausible phenomena contributing to the net force generation of a tire are the rubber-snow interaction, snow-snow interaction, snow braking force, bulldozing resistance and the digging force. The rubber-snow and the snow-snow interaction are the major source of traction on snow. The other plausible forces have comparatively less contribution but are important to be established for further understanding the tire traction on snow.

Accurate models are necessary to obtain reliable results. And with simulations being the heart of today's automotive industry, the models need to be simple enough so that it can be used with low processing power. Thus from an engineer's point of view, an analytically derived model is important for vehicle dynamics simulations. Also by adding more phenomena to our models, we can thus potentially understand more while keeping it as simple as possible.

In this thesis, we extend the common brush model to study the snow interaction and its effect on the net force generation. Further, by analytically deriving the quantities it was possible to connect tire design to vehicle performance, which can be essential for a tire manufacturer.

From the results obtained we see that the net effect of the derived tire model shows a good match to available measurement data. The model which includes the material properties can be thus potentially used on other loose surfaces with verification from test data.

Keywords: rubber-snow, snow-snow, digging force, bulldozing resistance, snow braking force, brush tire model.

Preface

The master's thesis was carried out in collaboration between the Vehicle Dynamics Group at the Chalmers University of Technology in Gothenburg, Sweden; and the Swedish National Road and Transport Research Institute (VTI) in Gothenburg, Sweden.

There are a number of people we would like to thank. First one being our supervisor Fredrik Bruzelius for his unconditional support and patience with our questions and queries during the length of this thesis. In addition we would like to thank Bengt J H Jacobson, our co-supervisor and examiner for his interest and advice during the thesis. A word of appreciation also goes out to Artem Kusachov, for his help in understanding the material shared, and to Alexandr Pralnikov of Cordiant who helped initiate this thesis.

Finally, we would like to thank our family, friends, fellow master's thesis students and our colleagues at the VEAS department at Chalmers, who have directly and indirectly helped us achieve this goal.

Göteborg, October 10, 2018

Nikhil Baliga & Gokul Gouda Hiregoudar

Nomenclature

Symbol	Description	Units
R_e/R_d	Effective rolling radius	m
a	Half the contact patch length of rubber bristle contact with surface	m
a_s	Half the contact patch length of snow bristle contact with surface	m
a_{cp}	Point at the end of the contact patch	m
c_{px}	Longitudinal bristle stiffness coefficient	-
c_{py}	Lateral bristle stiffness coefficient	-
μ_k	Isotropic friction coefficient	-
x_s	Breakaway point	m
ψ	Normalized slip (x, y)	-
σ_x^o	Limit slip	-
σ_y^o	Limit slip	-
F_z	Normal Load	kN
F_{x-rs}	Force offered in longitudinal direction for rubber to snow interaction	kN
F_{y-rs}	Force offered in lateral direction for rubber to snow interaction	kN
F_{x-ss}	Force offered in longitudinal direction for snow to snow interaction	kN
F_{y-ss}	Force offered in lateral direction for snow to snow interaction	kN
F_b	Force offered by snow in front of tyre	kN
F_{br}	Force due to bulldozing resistance on the tire side wall	kN
F_D	Force offered by digging action of the bristles	kN
h_o	Penetration depth	m
R_{le}	Reaction force from leading edge	kN
R_{cp}	Reaction force from contact patch	kN
H	Height of void	m
L	Length of contact patch	m
b	Width of contact patch	m
rvc	Ratio of void area and contact area	-
α	Contact length related to void surface	m
$\sigma_c(h_o)$	Compressive stress normal to tire surface	m^2
$\sigma(z_b)$	Stresses in compression in the tread block area	m^2
$\sigma(z_v)$	Stresses in compression in the void area	m^2
$\sigma(x_b)$	Stresses in compression in the tread block area	m^2
$\sigma(x_v)$	Stresses in compression in the void area	m^2
X_c	Destructive angle	deg
α'	Angle of approach	deg
$h_{buildup}$	Build up of material due to bulldozing	m^2
ϕ	Angle of repose	deg
c	Cohesion stress	Kg/m^2
ρ_o	Density	Kg/m^3
α_y	Lateral slip	-
σ	Longitudinal slip	-
λ	Wheel sinkage ratio	-
μ_s	Friction coefficient (snow)	-
μ_r	Friction coefficient (Rubber)	-
δ_i	Deflection of the bristle	m
V_x	Vehicle speed	m/s
ω *or* Ω	Wheel rotation speed	rad

Contents

1 Introduction

Tire is the only point of contact between the vehicle and the ground. It is through the tire's contact patch the forces are generated. The contact patch for a set of four tires is as large as an A4 sheet of paper. All the necessary traction required is dependent on the contact patch, which essentially becomes a problem during winter. With the roads susceptible to snowfall and a severe drop in temperatures, the friction levels available on the road surface drops, hence it is of utmost necessity to maximize traction.

Modeling the tires interaction on snow is very important to improve the tire performance on snowy roads. Snow as a material is complex and performing repeatable tests on it is hard due to the fast changing weather conditions. Due to the difficulty in measuring the snow mechanical characteristics, only a few notable attempts have been made according to the authors knowledge and two of these snow test data are used in this study and model.

To model the interaction on snow a conventional brush tire model cannot be used as it is derived under certain assumptions which are very different from that found in snow conditions. The results thus obtained gives unreliable results and is confirmed by measurements as seen in for example [2]. Thus a different approach needs to be used to model this interaction and is discussed in detailed further in the chapters.

1.1 Specification of issues under investigation

Various studies have been conducted which show that there are several forces that act during the interaction of a tire on snow. Apart from the obvious rubber - snow interaction, there are the snow - snow interaction, snow braking force, digging force and bulldozing force, which additionally aid or hinder traction capabilities as stated in papers [1] and [3]. All these forces are clearly discussed further in this report with their respective modelling approaches. By knowing the effect of these individual forces with a detailed model it was possible to gain an insight into the handling properties and the also tire design.

1.2 Research Objectives

The research objective here is to study the forces that act during the tire's interaction on snow and develop a vehicle dynamics model usable for handling, traction and braking simulations. Also, to further create a distinction on the forces, and to evaluate the contributing effect of each factor, with a goal to connect tire design parameters to vehicle performance.

1.3 Limitations

The research work is limited to,

- flat roads.
- only passenger car tires.
- tires with studs, or auxiliary chains around wheel will not be considered.
- the use of symmetrically designed tire treads, with the exception of the Christmas tree tread pattern.
- nominal tire pressures.
- not including rolling resistance of the tire (offered by the carcass). The resistance offered by the snow is still included.
- only snow on hard ground (such as asphalt), without the consideration of icy surfaces, soil under snow, ice bits on the snow, among others.
- only pure slip cases.

1.4 Deliverables

A list of deliverables are established and are as follows,

- literature survey on the topic of tire to snow interaction.
- tire model incorporating all the plausible phenomena for force generation based on our literature survey.
- validation of the model using test data from VTI.
- study on how various factors contribute to the overall force generation.
- technical report.

1.5 Methodology

With test data available from VTI, and with access to several technical paper databases, the information available on hand was beneficial to reach the intended goal of the thesis. The data available could only verify the net effects and not the individual contribution from each of the forces. This thesis was carried out with the participants working in-sync, with timely supervision meetings with Fredrik Bruzelius of Chalmers/VTI, and inputs from Alexandr Pralnikov of Cordiant, Russia.

A comprehensive literature survey on the topic of tires and snow was carried out to understand the problem at hand and to get a better understanding of a multi disciplinary modelling scenario. The vehicle dynamics model was developed in tandem and compared to the test results. MATLAB and Simulink as tools were used to develop and verify the model.

2 Snow

Very often the snow properties and its characteristics are ignored when tire modelling on snow is considered. However, it is very important to study snow as a material in order to understand the tire interaction. Snow being a non-solid surface is more complicated than asphalt and requires a detailed model which takes into account the snow properties to evaluate the interaction with a tire. The compression of the tire on snow and the ability to fill voids are some areas where knowing about snow properties becomes crucial. Thus, it is important to have snow test data which establish the measurable quantities such as density, internal friction angle, shear stress, etc that can be used in the models.

There are several factors that play a role in understanding snow as a material. Its hardness, type, density are directly related to the metamorphic process. The snow particles changes from flakes to granular particles as part of the densification process. The moisture content in the snow varies depending on the temperature and the environment. Additionally, the tire moving over the snow also changes the material properties and it is difficult to define an appropriate snow model.

Acknowledging the complexity of the snow, the snow properties considered in this report are based on two snow test data that was available for modelling through the initial literature survey. The tests are briefly explained in the following sections and the results from them are used in the model.

2.1 Types of Snow

Snow is made up of three different phases, viz. ice, water and air, with the water phase minimal at the subzero temperatures. The most common types of snow based on visual observation found on the roads are explained as per the author in [7].

2.1.1 Fresh Snow

It is the newly fallen snow on the ground which is free from mechanical loading or any tire rolling over it. This snow has little bonding between the snow particles and is very sensitive to loads and environmental changes, such as temperature. It has very little penetration resistance and can easily get compressed by even low loads.

2.1.2 Soft Packed Snow

The soft packed snow type is attained when a free rolling tire goes over the newly fallen snow and the entire tread pattern is imprinted on the snow.

2.1.3 Medium Packed Snow

When several passes of vehicle goes over the soft packed snow it leaves a partial tread marks on the surface. This is classified as Medium Packed Snow.

2.1.4 Hard Packed Snow

The hard packed snow type denotes that the snow is completely compacted on the road surface due to multiple passes of vehicles over medium packed snow. There is little or no tread pattern imprinted on the road as a consequence of surface hardness. This snow is characterized by increase in the strength of the inter-particle bonds and the snow density.

2.1.5 Slush (Melted Snow)

Slush is a mixture of the snow with high moisture content and behaves more like a fluid when compared to other snow types and usually occurs at zero and above temperatures.

The snow types as classified above give a good idea about the surface, but can not be used as a model input parameter. This is because there are no snow test data that use these terms and hence no accuracy of

results. The best possible way to continue with the modelling process is to classify the snow based on one particular category that is suitable to use as a model parameter. Thus in this study snow has been classified based on its age (sintering), which will be discussed further in the next section. Additionally, for the snow modelling case, we assume the vehicle to be run on hard packed snow as seen from the figure 3.1 where the tests were carried out. The necessary parameters such as internal friction angle, cohesion stress and penetration resistance are determined through available snow measurement tests which is discussed in the next section.

2.2 Snow Tests

To obtain the relevant parameters required for modelling, two measurement tests for snow are available. Rectangular Plate Loading Test data from [4] and Vane Cone Test data from [5].

2.2.1 Rectangular Plate Loading Test

It is important and critical to establish the relationship between the mechanical properties of snow and the depth of penetration under compression for snow modelling. For this purpose, the rectangular plate loading test on snow is performed by using a rectangular plate with a penetration speed of 3.7mm/sec and was carried out for snow collected during the snowfall. The freshly collected snow (D0) was sintered (aging the snow by maintaining the same temperature conditions) in the refrigerator at $-13^oC \pm 1^oC$ and D0, D1, D3, D7 and D14 are the different snow types used for the test. The numbers in snow types indicate the number of days stored (aged) in the refrigerator. A relationship is established between the penetration resistance $\sigma_c(h)$ and the penetration depth for different snow types and plotted as a graph. This relationship is further used in the model to calculate the tire's penetration into snow.

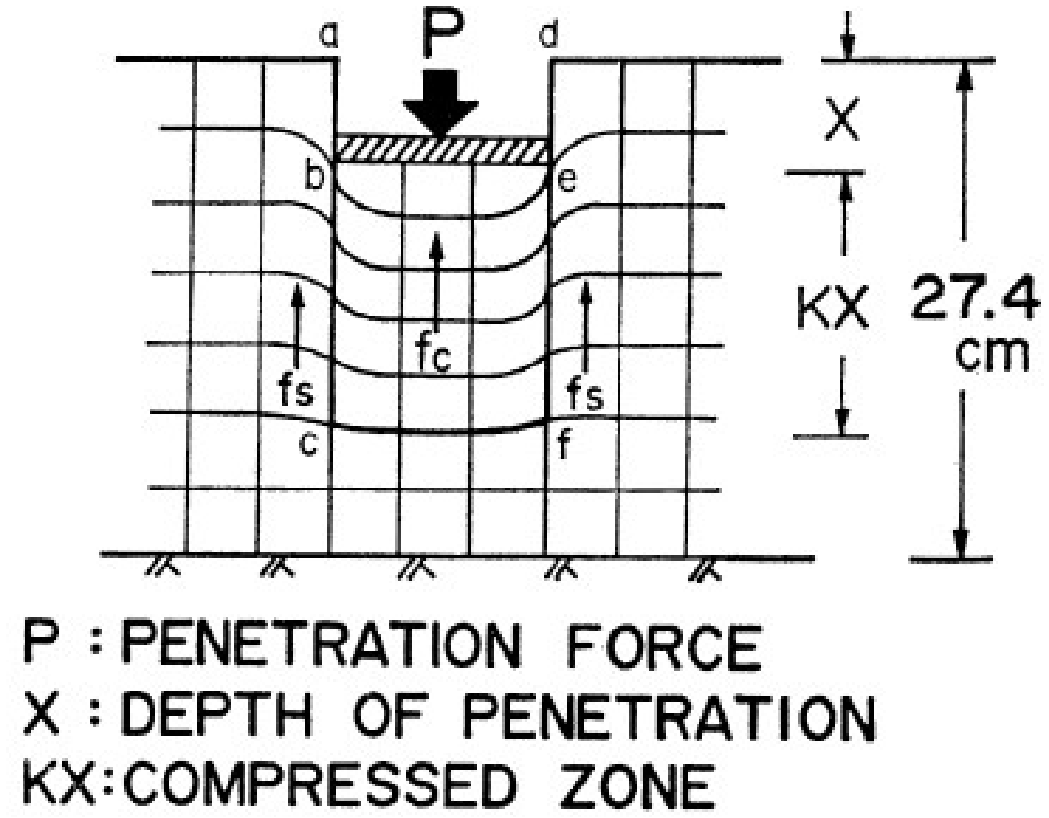

Figure 2.1: Rectangular plate loading test [4]

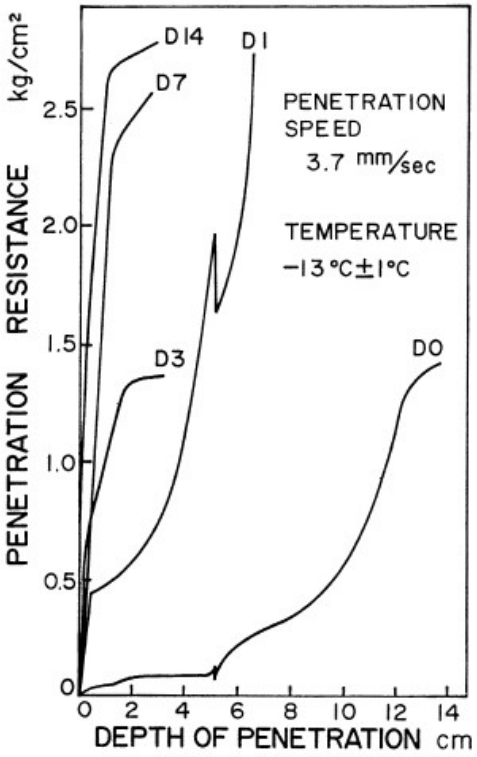

Figure 2.2: Penetration Resistance vs Penetration Depth [4]

2.2.2 Vane Cone Test

In this test, other necessary snow mechanical properties are obtained. The snow types considered are the same that were used in rectangular plate loading test. Here, a relationship is established between the shear stress (τ) and the normal stress (σ). From this relationship, mechanical properties such as cohesion stress (c) and internal friction angle (ϕ) are determined which are needed to model.

To give a brief about the test, the vane cone test is a method to determine the shear resistance of the snow. The test is carried out using a vane cone apparatus in the cold temperature room of -13^o C at the same temperature in which the the snow was aged. A snow box is filled with the same snow used in the rectangular plate test and at a constant penetration speed of 3.7 mm/sec the vane cone is pushed into the sample and the values are measured. The test is conducted on all snow types and a graph of shear stress v/s normal stress is plotted, from which the cohesion stress and the angle of internal friction is determined. The shear stress is a function of normal stress and is given as $\tau = \mathrm{f}(\sigma) = \mathrm{c} + \tan(\phi) * \sigma$.

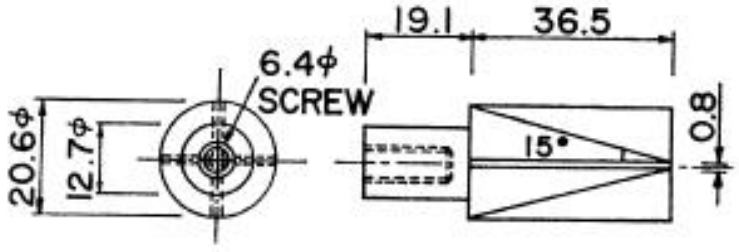

Figure 2.3: Vane Cone Apparatus [5]

Snow type	$\tau = f(\sigma) = c + \tan(\phi) * \sigma$	c (kg/m^2)	ϕ (degrees)
D0	$\tau = 4.3 + 0.418^*\sigma$	438.33	22.683
D1	$\tau = 6.1 + 0.214^*\sigma$	621.814	12.077
D3	$\tau = 8.8 + 0.245^*\sigma$	897.049	13.768
D7	$\tau = 17.3 + 0.348^*\sigma$	1763.507	19.188
D14	$\tau = 13.6 + 0.222^*\sigma$	1386.34	12.519

Table 2.1: Shear stress (τ) as a function of Normal stress (σ) for various snow types [8].

These tests have given an idea on how to utilize the material properties and have been subsequently used in modelling the interaction of a tire on snow for various snow types. The use of these results vary from a real world scenario of the actual snow properties, but can conclusively evaluate the various force interactions.

3 Tire Measurements

The mathematical model developed with physical motivation that includes all the plausible forces are compared with the test track measurements for two classes of unstudded winter tires. The measurement tests through which the model is evaluated were carried out by VTI using a BV12 mobile tire testing rig and is described in detail in [2] and [10].

Figure 3.1: Snow Test Surface [2]

3.1 Measurements

Longitudinal and lateral tests were carried out with over 9 sets of tires for each class of unstudded tires. A reference tire was used to track the surface changes and its measurements were collected every time a new type of tire was tested. All the unstudded tires used for measurements were worn by driving them for 100 km on asphalt.

The longitudinal brake tests were performed at a constant speed of 30kmph, with an over time linear increase of brake force. The test took around 4 seconds to perform, and was limited to track length and vertical oscillation excitations from the rig. The duration of 4 seconds was long enough for the slip curve to be framed as a steady state test and the slip values were gradually increased to obtain the slip stiffness accurately.

Figure 3.2: VTI's BV 12 Mobile Test Rig [15]

The lateral test was performed at the same speed of 30 kmph and swept from side to side by an angle of approximately 20 degrees for 35 seconds. A force measuring hub mounted on the rear of the mobile test rig developed by the VTI measured the forces acting on the tire in the longitudinal, lateral and vertical directions with a static vertical load.

With the objective of measuring many tires during the testing there was a trade-off on which was the most important one to measure. So for all the tires only the steering and braking case was measured. Also an offset was noticed from zero in the force-slip curves measured data. The offset is due to the measurement errors, partly form the tire and partly from the rig (offset from the sensors, incorrect rolling radius etc.). Determining or analyzing the offset of the measured data is not within the scope of the thesis and is not needed to develop the analytical model.

The analytical model being discussed in this report is based on the same condition of speeds, normal loads and steering excitations, with an assumption that the snow surface during the measurement test is similar to D7 snow (hard packed snow).

4 Tire Fundamentals

Before going into the details of a tire model, its important to know some background on passenger car pneumatic tires and their construction on a higher level. The general construction of a normal pneumatic tire is shown in figure 4.1.

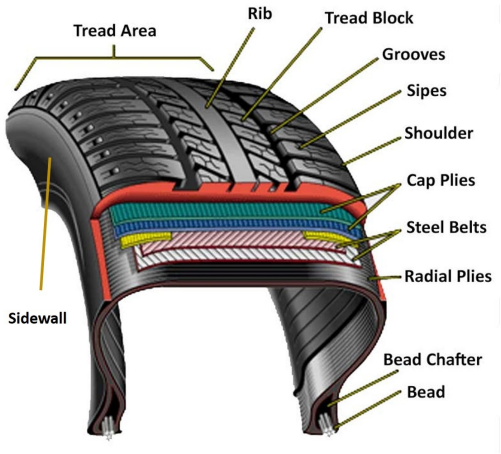

Figure 4.1: Tire construction and its components [11].

4.1 Types of Tires

In the Northern part of the world, vehicles driven on public roads are required by law to have winter tires during the winter seasons. Most Scandinavian countries run on winter tires from late October to early May to maximize traction for roads covered with snow and ice. The tires are classified based on legislation as summer tires and winter tires. Further, winter tires are differentiated between studded and non-studded winter tires. These tires are discussed further in the following sections.

4.1.1 Summer Tires

Most of the vehicle manufacturers equip their new vehicles with summer tires and are commonly referred to as performance tires. These tires increase the road holding performance during warm weathers when compared to winter tires. These tires have high bristle stiffness and the tread blocks are larger in size. Under colder conditions, the rubber tread compound tends to become inelastic and brittle which can result in permanent damage or high wear of the tires, as stated in [12]. Less regard of these tires is given to performance on ice and snow, as the in-elasticity and brittleness of the tread blocks at low temperatures do not maximize contact with the icy or snowy road surface.

4.1.2 Winter Tires

These tires are tailor made to increase performance in severe winter conditions. The rubber compound is very different from that of summer tires and it is very flexible and soft at extreme negative temperatures. Winter tires when compared to summer tires have an additional tread element known as 'sipes'. These sipes as seen in figure 4.2, are small carvings made on the tread blocks which is proved to be very essential in terms of grip on snow and ice. They divide the tread block into many more small elements thus maximizing rubber contact on the surface. Additionally winter tires have larger void ratios, which enable for better traction owing to snow - snow interaction. But an optimum void ratio is maintained to provide same traction on snow and ice. The tires marked with three mountain peaks and snow flake symbol indicates a winter tire and is designated only after meeting the winter performance criteria of having a snow traction index of 110 percent based on ASTM

F-1805 snow traction test standard. These tires are best suited for colder temperatures as they have much softer tread blocks, which maximizes contact on relatively softer road surfaces. Additionally, winter tires are further classified as Nordic winter tires, European winter tires and South European winter tires and are mainly based on the tread compound stiffness, design and the depth of sipes.

Figure 4.2: Summer and Winter Tires [Picture from Putney's Brake and Alignment]

4.1.3 Studded Tires

Studded tires are similar to winter tires having similar rubber tread compound but additionally fitted with pin like structures called 'studs' made up of ceramic or metal. Studs are mainly beneficial for traction on ice and also helps the driver compensate for the changes in friction levels, during fast changing weather conditions. These kind of tires are mainly used in the northern countries like Sweden, Norway, Finland and some part of Russia. Most of the countries have either banned the use of these tires or regulated its usage period on environmental grounds. With strong regulations in place, it is thus important to maximize grip and analyzing the sources of traction on snow and ice road surfaces without the aid of such studs.

Figure 4.3: Studded Winter Tires [Picture from Canadian off the grid]

4.2 Tire Kinematics

Tire kinematics are important for understanding the vehicle handling and force generation from the contact patch. In this section, the relevant definitions of tire kinematics are defined and introduced which are further used in the tire models and throughout the report. The vector components are denoted by an overhead bar i.e. $\bar{v}$.

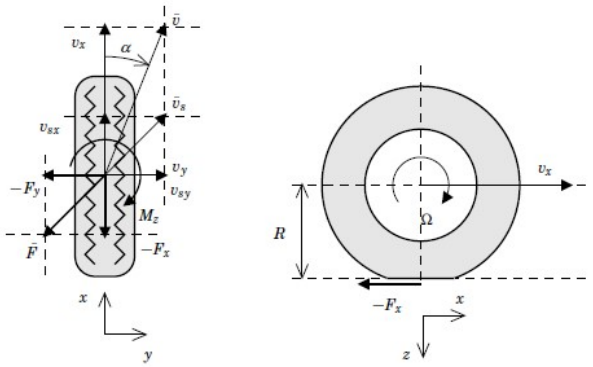

Figure 4.4: Tire Kinematics in cornering and braking conditions including the force vectors [13]

The wheel circumferential velocity is given as,

$$v_c = \omega R \tag{4.1}$$

The tire's effective rolling radius during pure rolling (when a small amount of torque is given to make the wheel move forward, i.e. Fx = 0) is given by,

$$R_e = \frac{v_x}{\omega} \tag{4.2}$$

The longitudinal slip for both driving and braking is given as,

$$\begin{aligned} Slip, \quad \sigma_x &= \frac{(R_e\omega - v_x)}{R_e\omega}; \quad driving \\ Slip, \quad \sigma_x &= \frac{(R_e\omega - v_x)}{v_x}; \quad braking \end{aligned} \tag{4.3}$$

Slip angle, the angle between the wheel heading direction and the wheel travel velocity which is given by,

$$\tan(\alpha_y) = \frac{v_y}{v_x} \tag{4.4}$$

Although not present in the tire model derived, equation 4.4 is presented for further understanding.

When a horizontal force is transmitted there is a relative motion of tire in the contact patch and this is known as slip velocity and is given by,

$$\bar{v}_s = (v_x - v_c, v_y) \tag{4.5}$$

The slip velocity direction is given by,

$$\tan(\beta) = \frac{v_{sy}}{v_{sx}} \tag{4.6}$$

The tires slips which are commonly used are defined by normalizing the slip velocity with a reference velocity are given as,

$$\bar{\sigma} = \frac{\bar{v}_s}{v_c} \qquad \bar{\kappa} = \frac{\bar{v}_s}{v_x} \qquad \bar{s} = \frac{\bar{v}_s}{v} \tag{4.7}$$

It is very common to mention the tire force as function of slip rather than as a function of slip velocity and therefore in the report the custom method is followed.

The forces and moments acing on a tire are based on the SAE J670e, 1976 standards and the same convention is followed.

In the SAE reference system, the longitudinal force F_x is along the wheel heading forward direction and lateral force F_y perpendicular to F_x and vertical force F_z downwards. The moments arising due to the forces acting on the tire M_x, M_y and M_z are along the x, y and z directions respectively. For vehicle handling purposes the forces acting on the planar longitudinal and lateral direction along with aligning torque are of big interest. The longitudinal force F_x is generated during the wheel driving and braking conditions. The lateral force F_y and self-aligning torque are generated when the wheel is cornering. The self-aligning torque arise due to the lateral planar force which is not acting exactly under the wheel centre but occurring at a distance offset from the wheel centre [13].

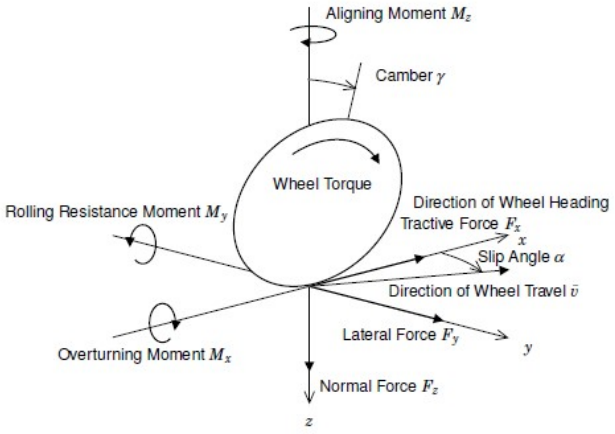

Figure 4.5: Tire Forces and Moments according to the SAE J670e standard [13]

4.3 Tire Models

There has been a vast research on modelling of tires which are motivated by understanding the physics involved. Several tire models are available that use an empirical approach to model tire forces. Although simple they have a large number of parameters that need to be inputted to give a good result. On the other hand, due to the complexity of the tire interaction with a snow surface it was important to develop a model with a physical approach. By having a physical approach more phenomena can be added and thus helping us gain more knowledge. Some of the common types of tire models used are classified as static (or steady state) and dynamic (or transient) tire models.

- Static tire models are further classified into physical (Brush tire model) and empirical tire model (Magic Tire formula).
- Some of the dynamic tire models are relaxation length model, LuGre model, stretched string model and SWIFT model.

Only the brush tire model will be used in modelling the interaction of a tire on snow, hence giving an analytical approach to arrive at an effective solution.

4.3.1 Brush Tire Model

The brush tire model is a physically motivated static tire model which has no dynamic states basically depicting steady state phenomena. This model is easy to understand, analyze, simple to implement and is a well-known

method to model tire forces.

This model takes into consideration certain assumptions, which gives rise to its validity. They are listed below.

- The model describes the force generated from the contact patch which is divided into the adhesive region and sliding region by a breakaway point, refer figure 4.6.
- The rubber in the contact patch region is divided into brush elements called as rubber bristles and the force is generated by these elements.
- Each bristle element stretches infinitesimally in the longitudinal direction but in the lateral direction it stretches only over the total contact length.
- The deformation of each bristle is not dependent on its neighbouring bristle regardless of the direction it is travelling.
- The rubber bristle is considered to be linearly elastic (factually rubber is not linearly elastic) and the deformation of each bristle is directly proportional to the shear force.
- The bristle enters the leading edge of the contact patch perpendicularly to the ground without any deformation.
- The bristle starts to slide when it exceeds a certain force level and is not capable of resisting it. The region where the rubber bristle is capable of supporting a certain force level is known as adhesive region. When the bristle begins to slide the region is known as sliding region and force generated in this region is independent of bristle deformation [14].

Adhesive region bristle forces
Consider a bristle in the adhesive region at a position x in Figure 4.7 from the center of the contact patch which is not sliding and is in contact with the road surface at,

$$x_r(x) = a - \int_0^{t_c(x)} v_x dt \tag{4.8}$$

$$y_r(x) = -\int_0^{t_c(x)} v_y dt \tag{4.9}$$

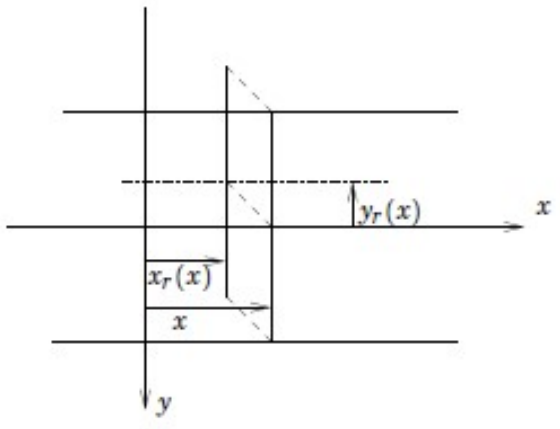

Figure 4.7: Bristle deformation in the contact patch both in longitudinal and lateral directions[13]

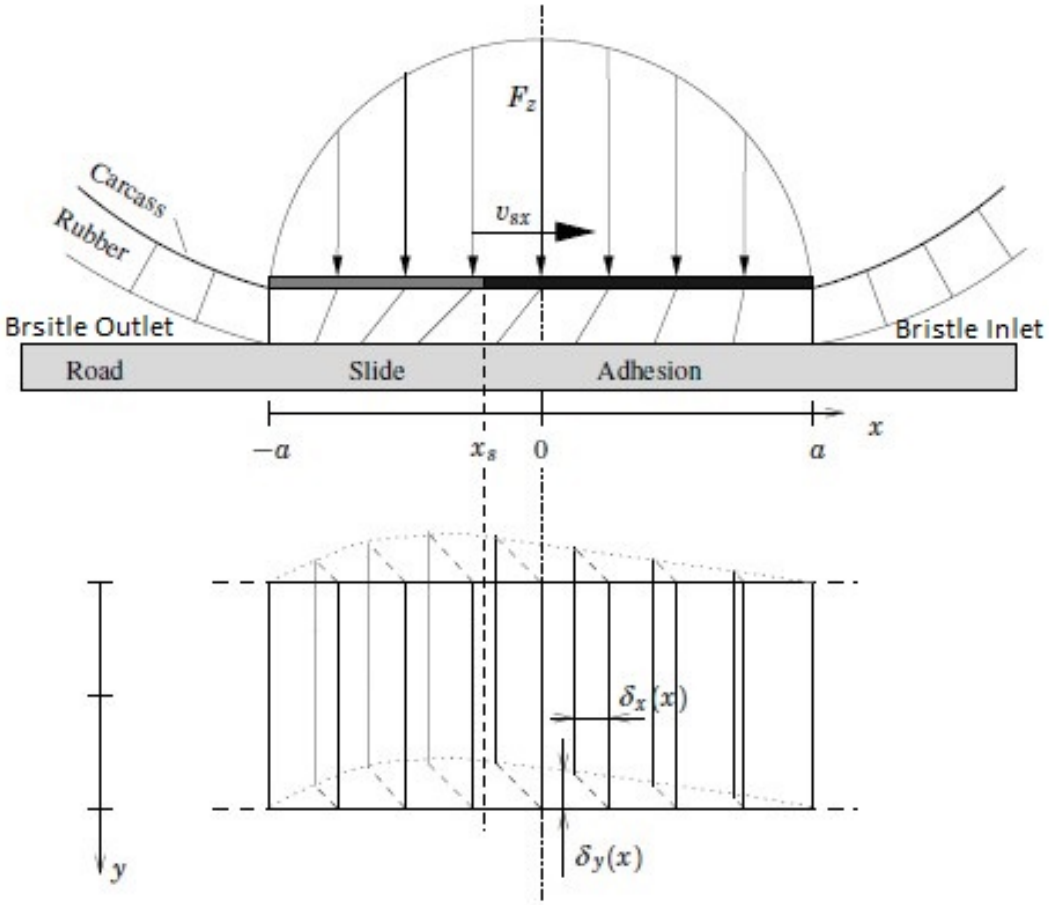

Figure 4.6: A typical Brush Model showing the bristle deformation in the adhesive and sliding region [13]

When the bristle enters the contact patch, there is a time lapse denoted as $t_c(x)$. When the bristle travels in the contact patch of the tire through the adhesive region in the interval i.e. $[0, t_c(x)]$ the velocities such as v_c, v_x and v_y are assumed to be constant. The position of the bristle is given as,

$$x = a - v_c t_c(x) \tag{4.10}$$

and,

$$t_c(x) = (a - x)/v_c \tag{4.11}$$

The bristle deformation in longitudinal and lateral direction can be written as,

$$\delta_x(x) = x_r(x) - x \tag{4.12}$$

$$\delta_y(x) = y_r(x) \tag{4.13}$$

Substituting equations (4.8) & (4.9) in (4.12) & (4.13) respectively, we get,

$$\delta_x(x) = -\frac{v_x - v_c}{v_c}(a - x) = -\sigma_x(a - x) \tag{4.14}$$

$$\delta_y(x) = -\frac{v_y}{v_c}(a - x) = -\sigma_y(a - x) \tag{4.15}$$

With the assumption of rubber bristle being linearly elastic, the deformation force for respective bristle deformations (4.12) and (4.13) is given in [13],

$$dF_{ax}(x) = c_{px} \ \ \delta_x(x)dx \tag{4.16}$$

$$dF_{ay}(x) = c_{py} \ \ \delta_y(x)dx \tag{4.17}$$

where c_{px} is the longitudinal bristle stiffness and c_{py} is the lateral bristle stiffness. The stiffnesses are per unit lengths. Integrating the deformation forces (4.16) and (4.17) over the entire adhesive region gives the total adhesive force,

$$F_{ax} = -\int_{x_s}^{a} dF_{ax}(x) = -c_{px}\sigma_x \int_{x_s}^{a} (a-x)dx \tag{4.18}$$

$$F_{ay} = -\int_{x_s}^{a} dF_{ay}(x) = -c_{py}\sigma_y \int_{x_s}^{a} (a-x)dx \tag{4.19}$$

The total adhesive force can be determined only when the breakaway point x_s is known. From the availability of static friction the size of the adhesive region can be determined. The elliptic constraint describes the static friction force which is given as,

$$\left(\frac{dF_{ax}(x)}{dF_z(x)\mu_{sx}}\right)^2 + \left(\frac{dF_{ay}(x)}{dF_z(x)\mu_{sy}}\right)^2 \leq 1 \tag{4.20}$$

By introducing the pressure distribution $dF_z(x) = q_z(x)$ and substituting (4.16) and (4.17) in (4.20) then the constraint of static friction can be expressed as,

$$\sqrt{\left(\frac{c_{px}\sigma_x}{\mu_{sx}}\right)^2 + \left(\frac{c_{py}\sigma_y}{\mu_{sy}}\right)^2}(a-x) \leq q_z(x) \tag{4.21}$$

The pressure distribution of a tires contact patch is highly complex. But for the purpose of modelling a general consideration is to use a uniform, parabolic or skew symmetric pressure distribution [13].

In this assessment, a parabolic pressure distribution is assumed which is given by,

$$q_z(x) = \frac{3F_z}{4a}\left(1 - \left(\frac{x}{a}\right)^2\right) \tag{4.22}$$

The breakaway point x_s is obtained by substituting the equation (4.22) in (4.21) with $x = x_s$ and removing inequality gives ,

$$x_s(\sigma_x, \sigma_y) = \frac{4a^3}{3F_z}\sqrt{\left(\frac{c_{px}\sigma_x}{\mu_{sx}}\right)^2 + \left(\frac{c_{py}\sigma_y}{\mu_{sy}}\right)^2} - a \tag{4.23}$$

The normal force acting in the sliding region is given as,

$$F_{sz} = -\int_{-a}^{x_s} q_z(x)dx = F_z\psi^2(3-2\psi) \tag{4.24}$$

However, the bristles are assumed to slide over the contact patch, once the limit slip values are reached, and is given by,

$$\sigma_x^o = \frac{3F_z\mu_{sx}}{2a^2c_{px}} \tag{4.25}$$

$$\sigma_y^o = \frac{3F_z\mu_{sy}}{2a^2c_{py}} \tag{4.26}$$

The normalized slip is given as,

$$\psi = \sqrt{\left(\frac{\sigma_x}{\sigma_x^o}\right)^2 + \left(\frac{\sigma_y}{\sigma_y^o}\right)^2} \tag{4.27}$$

The total tire forces in the longitudinal and lateral direction are obtained by adding the adhesive region and sliding region forces and is given by,

$$F_x = F_{sx} + F_{ax} = -\cos(\beta)\mu_k F_z\psi^2(3-2\psi) - 2a^2c_{px}\sigma_x(1-\psi)^2 \tag{4.28}$$

$$F_y = F_{sy} + F_{ay} = -\sin(\beta)\mu_k F_z\psi^2(3-2\psi) - 2a^2c_{py}\sigma_y(1-\psi)^2 \tag{4.29}$$

The final form of the longitudinal and lateral force generation as given in equations 4.28 and 4.29, incorporate isotropic friction in both the directions for the sake of simplicity.

4.3.2 Self-Aligning Torque

Emphasis is not given currently to model the self-aligning torque. Contribution of rubber-snow and snow-snow interaction to the aligning moment is evaluated in [2], and has not been discussed further in this report.

5 Interaction of a Tire on Snow

In addition to the obvious rubber - snow friction, there are several other forces that aid or hinder traction on a snow surface. This chapter discusses these forces in detail together with the method they have been modelled with. A representation can be seen in the figure 5.1.

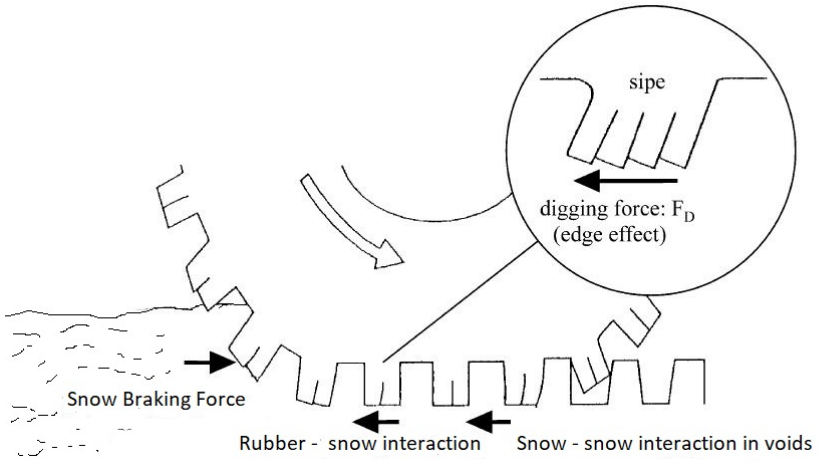

Figure 5.1: Force generation on a snow surface [1]

5.1 Rubber to Snow Interaction

The force generated is from the tire tread blocks that is in contact with the snow surface. To model this, the tire brush model as explained in section 4.3.1 is used. Using the final form of the tire brush model equation in the longitudinal and lateral direction, we get,

$$F_{x-rs} = F_{sx} + F_{ax} = -\cos(\beta)\mu_k F_z \psi^2(3 - 2\psi) - 2a^2 c_{px}\sigma_x(1-\psi)^2 \tag{5.1}$$

$$F_{y-rs} = F_{sy} + F_{ay} = -\sin(\beta)\mu_k F_z \psi^2(3 - 2\psi) - 2a^2 c_{py}\sigma_y(1-\psi)^2 \tag{5.2}$$

This model requires friction coefficient (μ_k) values and the associated lumped rubber stiffness coefficients (c_{px} & c_{py}) values. These are derived from curve fitting to VTI's test results and are tabulated in table 5.1.

Tire Type	Friction Coefficient (μ_k)(−) (rubber to snow)	Longitudinal Stiffness Coefficient (c_{px})(−) (rubber to snow)	Lateral Stiffness Coefficient (c_{py})(−) (rubber to snow)
Nordic Tire	0.3105	9.2756	8.2018
European Tire	0.3095	12.6121	8.1077

Table 5.1: Friction and stiffness coefficients for rubber to snow interaction

5.2 Snow to Snow Interaction

Passenger car tires have tread patterns engraved on them. The main reason is to move water and dirt fragments from the road surface, thus maximizing traction. Similarly in the case of a winter tire, tires are equipped with tread patterns and additionally with sipes. But during a tire's interaction on snow, the voids in the tire gets filled up with snow. This snow build up in the voids is proved to maximize traction further by shear contact with the snow surface, as discussed in [2].

5.2.1 Modelling

As described in the paper [1], the traction force arising is a function of the snow properties and the interaction is physically motivated from a material perspective. This approach though valid is impractical for vehicle dynamics simulations.

Hence, a tire brush model approach similar to the one used for rubber - snow interaction is hence used to model this force generation and is taken from [2]

To understand the "snow tire" brush model better, a preliminary assumption is laid forward. It is assumed that the snow bristles formed in the voids is stiff enough to have an adhesive region and sliding region of its own. The differences however using this double interaction brush model (Rubber tire brush model and snow tire brush model) are,

- The need to have different breakaway points for rubber and snow, since they have varying friction co-efficient.
- The interaction between rubber-snow, and snow-snow have different frictional coefficients and bristle stiffness coefficients.
- The resultant forces and moments can be gathered, by adding the forces from the rubber and snow bristles.

But validating such a model requires additional assumptions. They are,

- The snow bristles when formed are assumed to be elastic.
- The Snow bristles are thrown out of the voids at the end of the contact patch, making way for new snow bristles to be formed every tire rotation.
- The rubber and the snow bristles are arranged symmetrically in the lateral direction.
- The snow bristles movement are independent of the movement of the rubber bristles.

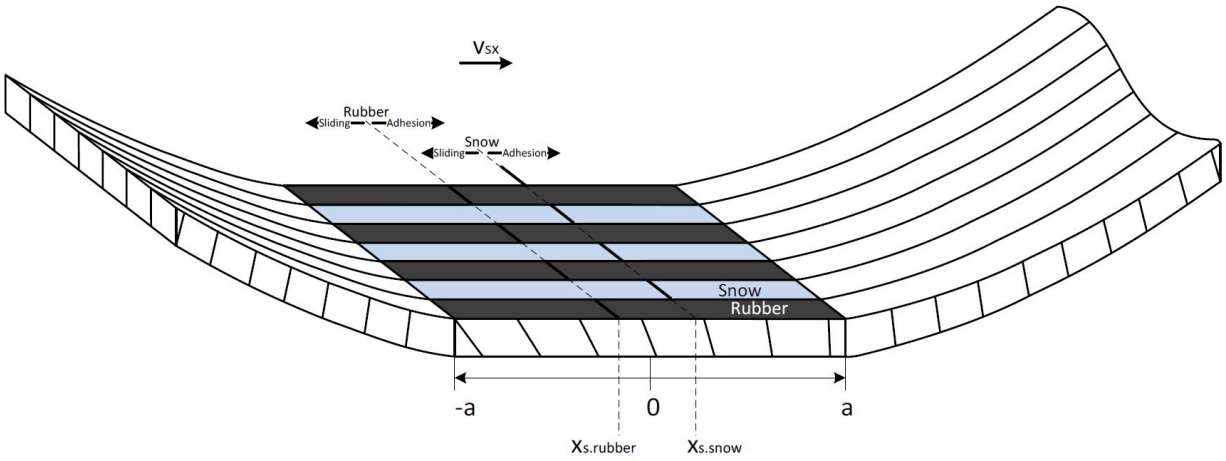

Figure 5.2: Schematic of a double interaction model [2]

Thus the force generation from snow - snow interaction is given by the equations 5.3 and 5.4. The only difference being that the lumped snow stiffness coefficients (c_{px} and c_{py}) and friction coefficients (μ_k) are different for snow - snow interaction. This is tabulated in table 5.2 and the values are derived from curve fitting from VTI's test results.

$$F_{x-ss} = F_{sx} + F_{ax} = -\cos(\beta)\mu_k F_z \psi^2(3-2\psi) - 2a_s^2 c_{px}\sigma_x(1-\psi)^2 \tag{5.3}$$

$$F_{y-ss} = F_{sy} + F_{ay} = -\sin(\beta)\mu_k F_z \psi^2(3-2\psi) - 2a_s^2 c_{py}\sigma_y(1-\psi)^2 \tag{5.4}$$

Tire Type	Friction Coefficient (μ_k)(−) (snow to snow)	Longitudinal Stiffness Coefficient (c_{px})(−) (snow to snow)	Lateral Stiffness Coefficient (c_{px})(−) (snow to snow)
Nordic Tire	0.2103	1.4637	0.9697
European Tire	0.185	1.2920	0.9697

Table 5.2: Friction and stiffness coefficients for snow to snow interaction

It is to be noted that, the μ_k, c_px and c_py appears as different numerical values for the different parts of the contact in the rubber to snow and snow to snow interaction, see table 5.1 and 5.2. Note specifically that μ_k is not the physical friction coefficient as it was in the single contact model, but instead a scaling, assuming a certain, fixed but unknown, distribution of the total F_z between the two parts. This leads to that the F_z in the formula is the total F_z for the wheel, not specific for each contact part.

An additional flexibility is given to this model by calculating the time needed to fill the voids with snow. This is then translated into the region of the tire's contact patch to calculate the point at which the snow bristles provides traction. By finding this distance, the force generated by the snow bristle is substituted in equations 5.3 and 5.4 to give the total force generation in the longitudinal and lateral directions. The time needed to fill the void is assumed to be the same for both a traction case and a braking case, although they might subtle changes between these cases.

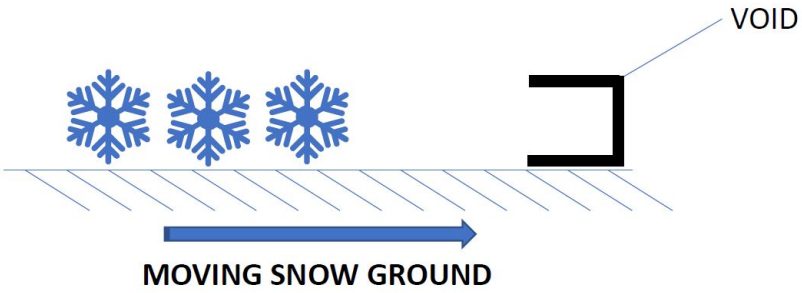

Figure 5.3: Schematic of a void fill model

To calculate the above, a simple model as shown in figure 5.3 is used. The model takes into assumption that the void is stationary and the surface is moving with a certain velocity. The flow rate is then calculated by the equation,

$$Q = \rho A V_x \tag{5.5}$$

The time needed to fill the void is then calculated by,

$$t_{void} = \frac{V_x}{Q} \tag{5.6}$$

Upon calculating the time, and translating into the tire's contact patch, the distance at which the snow bristle is formed is calculated.

$$d_{snowbristle} = V_x * t_{void} \tag{5.7}$$

As seen in the figure 5.4, the snow bristle provides traction a modest distance after the rubber bristle provides traction.

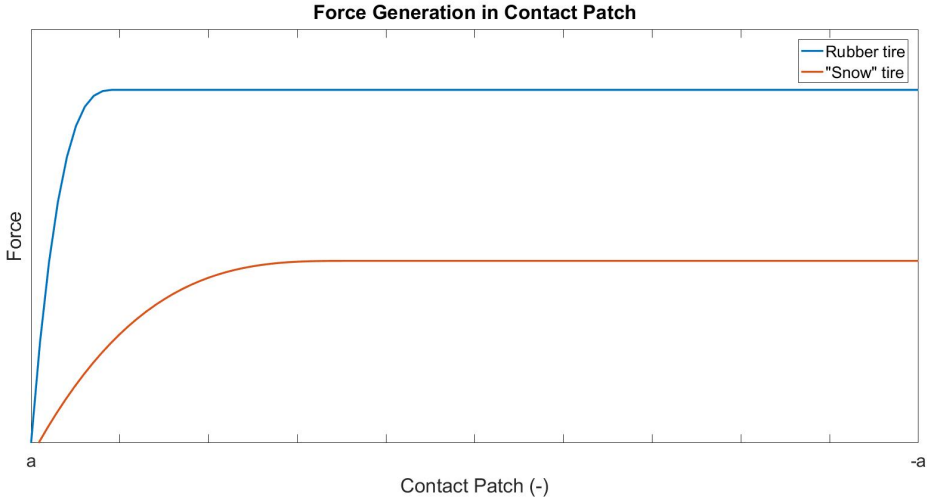

Figure 5.4: Force Generation in Contact Patch

5.3 Snow Braking Force

When a tire rolls over a soft surface like snow or soil, the normal load on the tire compresses the snow at the leading edge and in the area of the tire's contact patch. This causes a step in front of the tire which resists its forward motion. An illustration of this can be seen in figure 5.5.

The compression of the snow happens in two sections as discussed in[1]

- Compression due to the pressure from the tread blocks
- Compression due to the pressure from the void area, only after it has been filled above and beyond the tires void depth.

Developing a model to evaluate such a phenomena are based on certain assumptions and are listed below.

- The contact patch size is assumed to be rectangular under static and dynamics conditions.
- The voids cross section is rectangular.
- The snow compression in the depth direction is determined by the calculated penetration depth.
- The snow density beneath the block and the void area is determined by the compression in the depth direction.
- The normal load is static.

5.3.1 Modelling

The model used is from [1] and as mentioned above compression happens in two sections in the leading edge. Thus when the height of snow is more than the void depth, compression happens due to the pressure at both the face of the tread block area and in the void area. And when the height of snow is less than the void depth, compression happens only due to the pressure at the tread block area.

The penetration depth (h_o) is thus calculated by force equilibrium between the tire normal load (F_z) and reaction force from the snow in the leading edge (R_{le}) and in the contact patch (R_{cp}) as seen in figure 5.5.

To calculate the reaction force from snow, the areas of the contact patch and leading edge are considered.

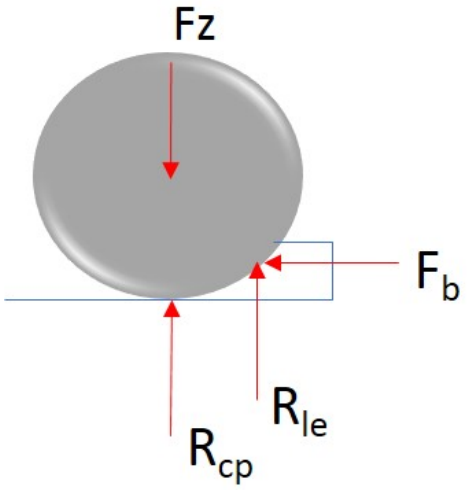

Figure 5.5: Snow Braking Force Evaluation

To calculate the reaction force from snow, the areas of the contact patch and leading edge are considered. Solving for force equilibrium, we arrive at,

If h_o<H,

$$F_z = Lb\sigma_c(h_o)(1 - r_{vc}) + bl(1 - r_{vc})\sigma(z_b) \tag{5.8}$$

If $h_o \geq$H,

$$F_z = Lb\sigma_c(h_o)(1 - r_{vc}) + \sigma_c(h_o) - \sigma_c(H) + bl(1 - r_{vc})\sigma(z_b) + b\alpha r_{vc}\sigma(z_v) \tag{5.9}$$

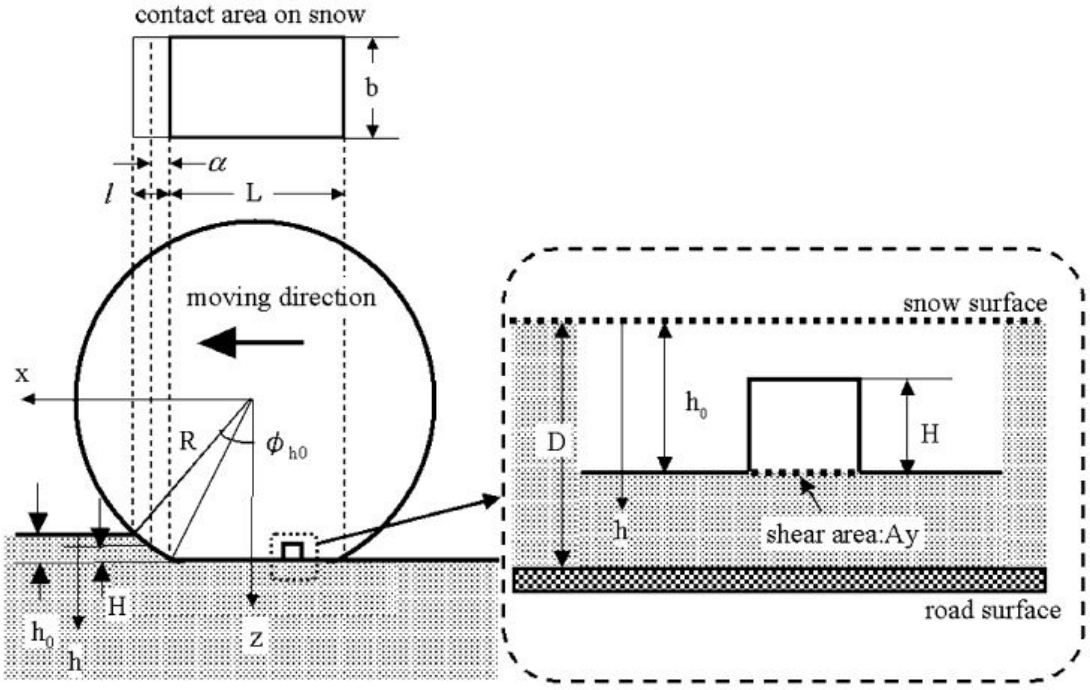

Figure 5.6: Snow Braking Force Analytical Model [1]

The stresses in the z - direction in the tread block and void area is calculated using,

$$\sigma(z_b) = \frac{1}{l}\int_{\frac{L}{2}}^{\frac{L}{2}+l} \sigma_c(h_o)cos(45)dx \tag{5.10}$$

$$\sigma(z_v) = \frac{1}{\alpha}\int_{\frac{L}{2}}^{\frac{L}{2}+\alpha} \sigma_c(h)cos(45)dx \tag{5.11}$$

where,

$$h = \sqrt{(R^2 - x^2)} - Rcos(\phi_{h_o}) \tag{5.12}$$

Upon solving the equations 5.8 or 5.9, the penetration resistance ($\sigma_c(h_o)$) is determined. Using ($\sigma_c(h_o)$), the corresponding depth of penetration is calculated based on the rectangular plate loading test data, as described in section 2.2.1.

The snow braking force thus generated due to the tire rolling over the step created in front of the leading edge is thus given by, [1]

When h_o<H,

$$F_b = h_o b(1 - r_{vc})\sigma_{xb} \tag{5.13}$$

When $h_o \geq$H,

$$F_b = h_o b(1 - r_{vc})\sigma_{xb} + (h_o - H)br_{vc}\sigma_{xv} \tag{5.14}$$

where the stresses in the x - direction in the tread block and void area is calculated using,

$$\sigma(x_b) = \frac{1}{h_o}\int_0^{h_o} \sigma_c(h)cos(45)dz \tag{5.15}$$

$$\sigma(x_v) = \frac{1}{h_o - H}\int_0^{h_o - H} \sigma_c(h)cos(45)dz \tag{5.16}$$

where,

$$h = z - Rcos(\phi_{h_o}) \tag{5.17}$$

Using this model, snow depths of 5mm to 30mm for different load cases are calculated. Figure 5.7 shows the result for one of the cases, and proves the predictability of the model. The 4kN load provides highest snow braking force due to its high penetration into the snow surface. Also seen in the bar graph, the D14 snow for a 4KN load was the only load case to compress into the hard (D14) snow, thus obtaining a snow braking force. Additional plots for the snow braking force for various snow depths can been found in section 10.

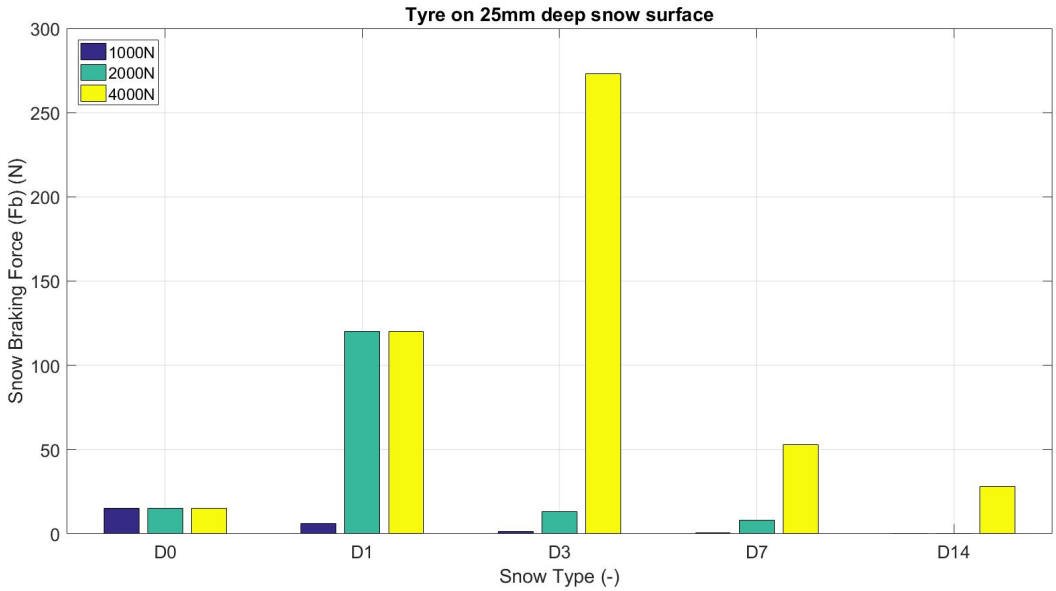

Figure 5.7: Snow Braking Force (F_b) on 25mm snow for various normal loads (F_z)

5.4 Bulldozing Resistance

Bulldozing resistance is the force acting on the tire side wall during a steering manoeuvre or during lateral slip. The force acting is a result of penetration of the tire into the snow surface. The penetration of the tire is calculated using the same relation as described in section 5.3, snow braking force. The amount of penetration of the tire into the snow, followed by lateral slip, dictates the force acting on the tire side wall.

To calculate this resistance force, a model given analytically by the Hegedus's estimation method is used. This method as described in [3] is mainly developed for tire-soil interaction. Though the physical properties, mechanical properties, and behaviour of snow is different from that of soil, the Hegedus's estimation method takes into account the mechanical properties of the material. By using the mechanical properties of snow from the vane cone test data in section 2.2.2, the model was extended for use on snow. This model takes into account material properties like the internal friction angle, density, cohesion stress, which is gathered from the vane cost test and is tabulated for various snow types in table 2.1.

Figure 5.8 shows the material build up on the outer sides of the tire and figure 5.11 shows the force that acts on the tire side wall. The bulldozed material on the sides is due to the angle of repose of the material, defined in [16] as the "steepest angle of descent or dip relative to the horizontal plane to which a material can be piled without falling."

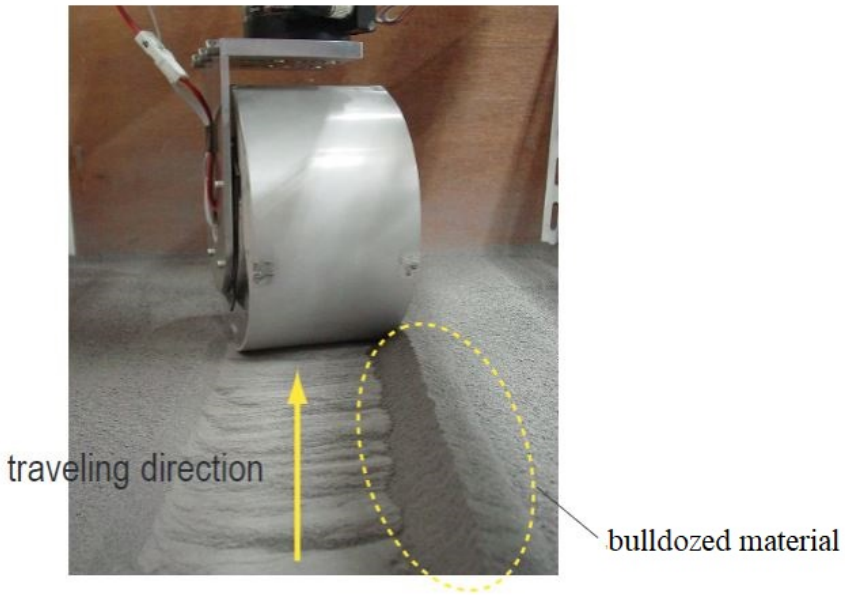

Figure 5.8: Bulldozing Representation [3]

5.4.1 Modelling

According to Hegedus's estimation method, the bulldozing resistance R_b is generated per unit width of the blade when the tire moves on the snow in the lateral direction. The blade moves with an angle of approach $\alpha^{'}$, that can be associated to the camber angle of the wheels.

The destructive angle X_c is formed linearly at the contact of the tire to the snow and defines the bulldozed area. h_0 is the penetration depth of the tire into the snow and $h_{buildup}$ is the snow which is swelled due to the bulldozing action.

The angle of repose of snow 'ϕ' is assumed to be same as the internal friction angle of the snow.

c is the cohesion stress and ρ_s is the density of the snow. The bulldozing resistance is thus determined from the following equations,

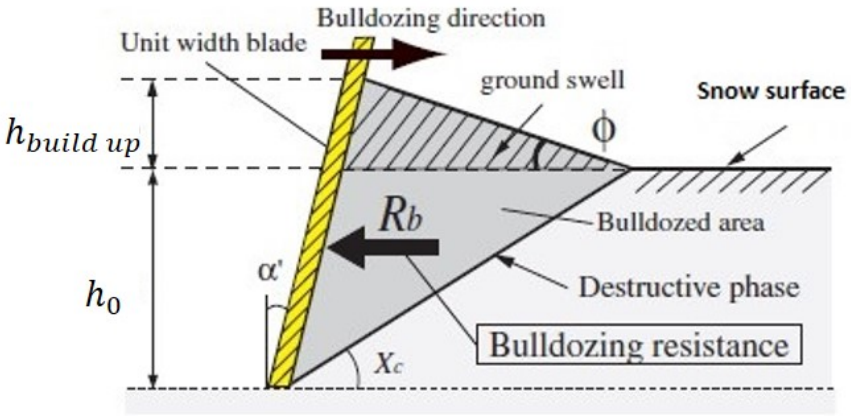

Figure 5.9: Hegedus' Estimation Method [17]

When $\alpha^{'} \neq 0$,

$$R_b = \alpha_y \left\{ \frac{\cot(X_c) + \tan(X_c + \phi)}{1 - \tan(\alpha') \tan(X_c + \phi)} \left[h_0 c + \frac{1}{2} \rho_s h_0^2 \left\{ (\cot X_c - \tan \alpha^{'}) + \frac{(\cot X_c - \tan \alpha^{'})^2}{\tan \alpha' + \cot \phi} \right\} \right] \right\} \tag{5.18}$$

When $\alpha^{'} = 0$,

$$R_b = \alpha_y \left\{ \{\cot(X_c) + \tan(X_c + \phi)\} \left[h_0 c + \frac{1}{2} \rho_s h_0^2 \left\{ (\cot X_c) + \frac{(\cot X_c)^2}{\cot \phi} \right\} \right] \right\} \tag{5.19}$$

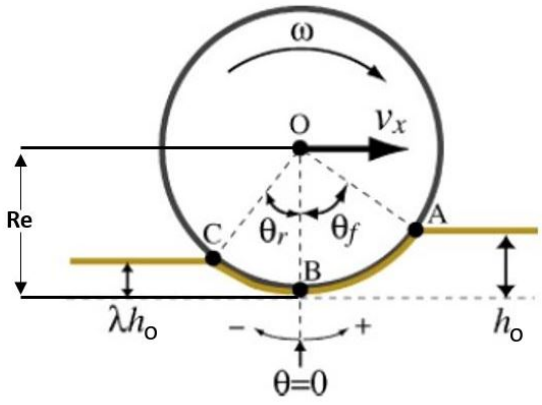

Figure 5.10: Wheel contact angles on snow [17]

$$\theta_f = \cos^{-1}\left(1 - \frac{h_0 + h_{buildup}}{z}\right) \tag{5.20}$$

$$\theta_r = -\cos^{-1}\left(1 - \frac{\lambda(h_0 + h_{buildup})}{z}\right) \tag{5.21}$$

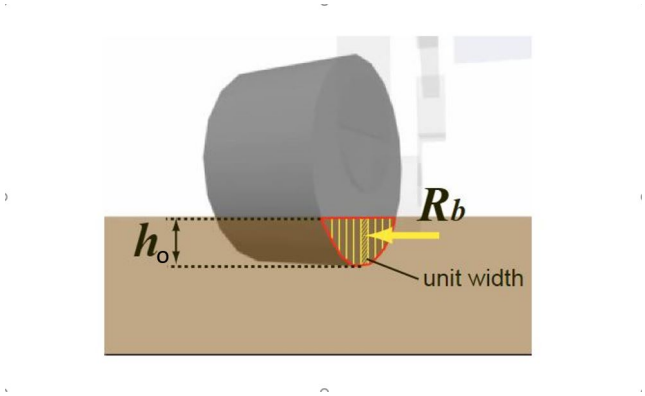

Figure 5.11: Bulldozing resistance on the tire side wall [17]

Assuming the wheel sinkage ratio λ to be 1, the snow accumulated on the side wall gives θ_r equlas θ_f.

The snow build up on the tire sidewall during lateral slip is included in the Hegedus's estimation method and is geometrically expressed as,

$$h_{buildup} = \frac{h_0(\cot X_c - \tan \alpha^{'})}{\tan \alpha' + \cot \phi} \tag{5.22}$$

The destructive angle is approximated as,

$$X_c = 45^o - \frac{\phi}{2} \tag{5.23}$$

Finally, the bulldozing resistance F_{br} on the tire side wall is given by,

$$F_{br} = \int_{\theta_r}^{\theta_f} R_b(R_e - R_e.\cos\theta)d\theta \tag{5.24}$$

Using the equations, the bulldozing resistance for all snow types viz. D0, D1, D3, D7 and D14 for different penetration depths are determined. The bulldozing resistance is considered to increase linearly over the entire slip range as the saturation point of the snow build up is not included in the model.

Additionally, the tire tread design is considered not to have any effect during bulldozing in the lateral direction.

Figure 5.12, shows the effect of bulldozing resistance for a penetration into 5mm of snow. As it can be seen, the resistance increases with slip and is very dependent of the internal friction angle of the material, thus showing D7 snow to be the highest contributor.

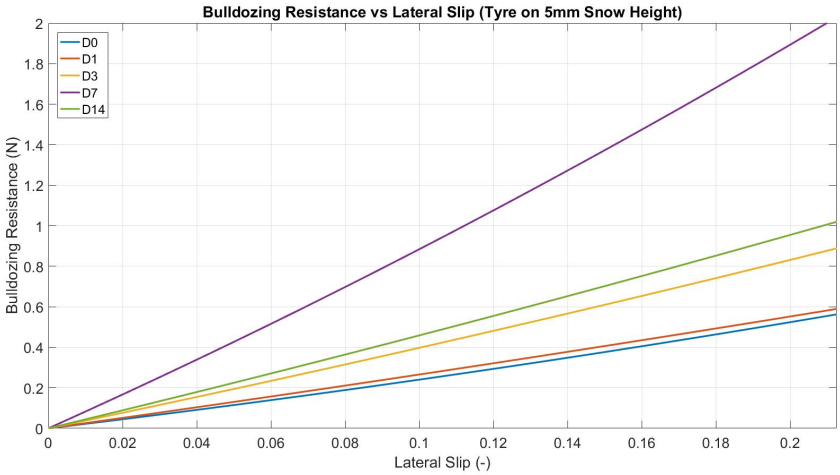

Figure 5.12: Bulldozing Resistance vs Lateral Slip

5.5 Digging Force

The digging force is the force generated by the tread blocks edges or sipe edges as described in [1]. The edge, shaped as a "claw" as shown in figures 5.13 and 5.14, penetrates into the underlying snow layer thus generating an additional force towards traction. This "claw" is assumed to be formed due to the softness of the tread block combined with the sipes on the tread blocks, which when deformed gives this shape. This phenomena contributes towards force generation both in the longitudinal and lateral direction, due to the edge penetrating into the snow surface. Before modelling this, understanding digging as a phenomenon is important. Digging occurs in three phases as described in [18]. Extending this phenomena to a tire tread block, we have,

- Phase 1 - Penetration of the edge into the underlying snow layer.
- Phase 2 - Plowing of the edges through the sliding region of the tire's contact patch.
- Phase 3 - Excavation or removal of snow from the contact patch.

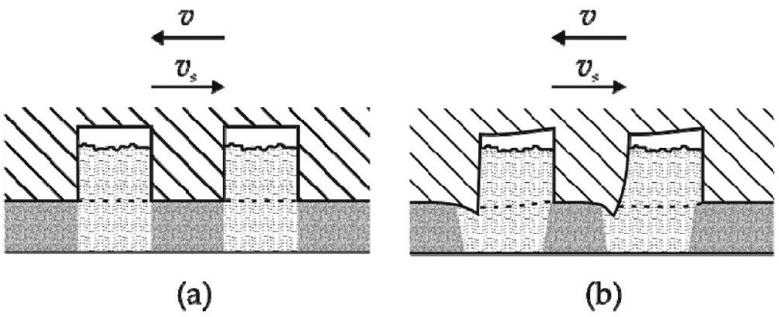

Figure 5.13: Digging of tread blocks edges into the snow [19]

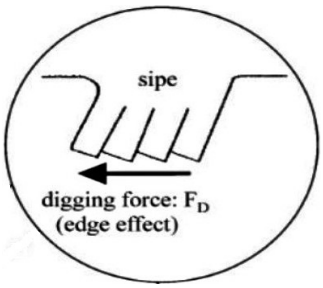

Figure 5.14: Edge Effect Representation [1]

Before understanding how this is modelled, it is important to put forth certain assumptions to understand the phenomenon better.

- The "claw" is assumed to be formed (phase 1) at high load according to the parabolic pressure load distribution and acts in the sliding region of the tire brush model.
- This effect is assumed to act over the whole sliding region.(phase 2)
- Phase 3 of the digging process acts towards the end of the contact patch.

5.5.1 Modelling

Phase 1 - Penetration

With the assumptions stated in the previous section, a further assumption that this edge or "claw" penetrates to a depth of 1.5mm into the underlying snow layer. This assumption is based on the literature survey of

papers discussing digging force. Although a valid number is not present through experiments, a conservative assumption of 0.15 cm is a start to evaluate this force.

Phase 2 - Plowing

The "claw" penetration into the underlying snow layer, plows through the entire sliding region and is modelled similar to bulldozing resistance as described in detail in section 5.4. This is again highly dependent of the type of snow and can seen in the figure 5.15. The internal friction angle of the snow as discussed chapter 2, is critical to the force being generated. This force generation is considered constant over the whole slip range, as the penetration of the "claw" with increase in slip cannot be established. It is also assumed that this "claw" penetrates to the same depth on all the different snow types discussed.

It is important to note that the bulldozing resistance model used takes into account snow build up. This model in the digging force also takes into consideration of this build up, whose effect is small and the force offered can be accounted to the snow compression that occurs between tread blocks during plowing.

$$F_{diggingphase2} = \int_{x_s}^{-a} R_b \;\; b \tag{5.25}$$

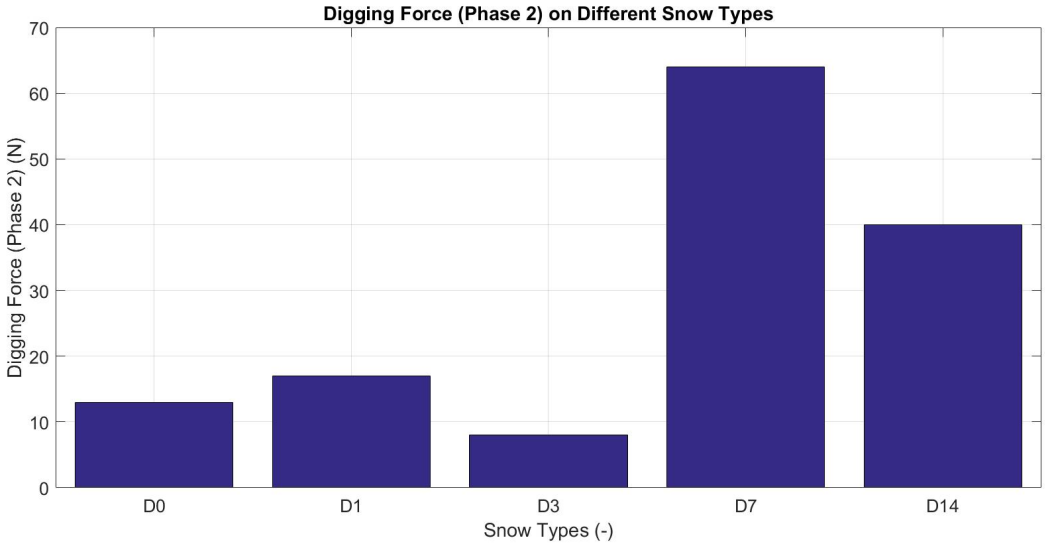

Figure 5.15: Digging Force (Phase 2)

Phase 3 - Excavation/Removal

The final phase of the digging process, occurring at the end of the tire's contact patch is modelled based on Hooke's law. Due to the speed difference of the bristle attached to the carcass and the bristle in contact with the snow surface, longitudinal deflection of the tread block exists. When the force required to sustain deflection is low (end of contact patch), the tread block is assumed to move back to its normal position, thus generating a force. Though small it has been evaluated. The set of equations to calculate this effect is given below and is taken from [20].

The deformation of the brush element is given by,

$$\delta_i = x_{ci} - x_{ri} = \int_0^t V_x - \Omega R_d dt \tag{5.26}$$

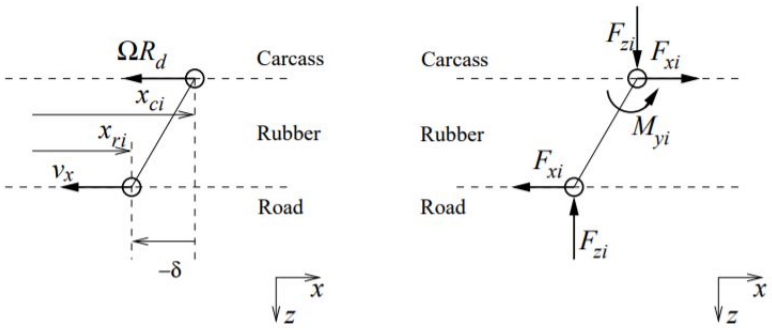

Figure 5.16: Bristle Representation [20]

With an assumption that rubber deforms linearly, the force generated by the amount of deformation of the bristle is given by Hooke's law. The force is integrated between distance 'b_x', a point at the end of the contact patch; and '-a', at the end of the contact patch.

$$F_{xi} = \int_{a_{cp}}^{-a} k\delta_i \tag{5.27}$$

Although the bristle deforms linearly, the deformation of the bristle is limited by the road surface and tire friction. The maximum deflection is given by [20],

$$\delta_{i,max} = \frac{\mu F_z}{k} \tag{5.28}$$

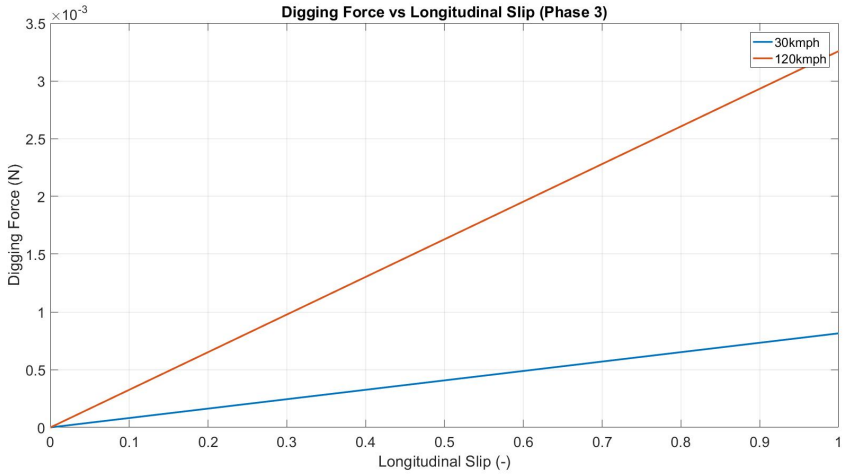

Figure 5.17: Digging Force (Phase 3)

As seen in the figure 5.17, increasing speed increases the deflection. Thus generating a relatively higher force.

An additional assumption is considered for the phase 3 of digging. Below, is an illustration of the bristle orientation during a traction and braking case. We assume that the force developed by the phase 3 action does not aid during a braking case. This is due to the orientation of the bristle and the snow build up in the voids. Thus assuming that the bristle will continue undeformed until it exits the contact patch. Finally, the total digging force (F_D) is a combination of these three phases as discussed above.

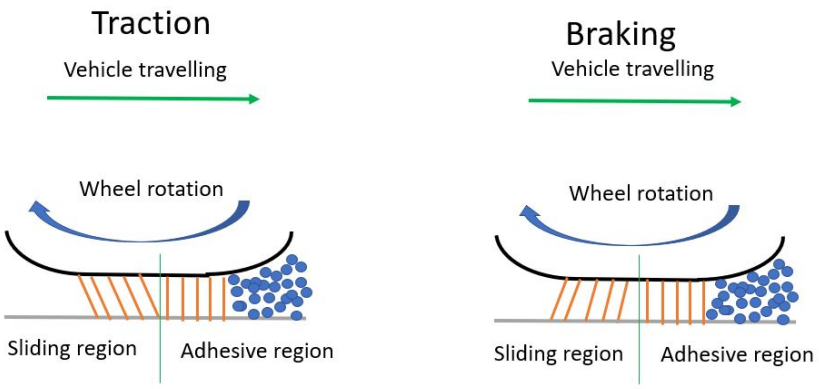

Figure 5.18: Digging Force (Phase 3) Illustration

6 Results

In this chapter, the models as discussed in the previous chapter are combined and compared to the test results. Before looking at the results it is worthy to note three terms that have been used in the chapter. The first one being the multi interaction model, which captures all the force interaction as discussed in the previous chapter. The second one being the double interaction model, which takes into account only rubber - snow interaction and snow - snow interaction and the final one being the single interaction model, which takes into account only rubber - snow interaction.

The single interaction model (conventional brush model) and the multi interaction model are compared to the test results in both the longitudinal and lateral directions. Two types of tires have been evaluated, Nordic tires and European tires.

These tire models additionally are also used to carry out vehicle dynamics simulations to further validate results for both the longitudinal and lateral directions. All of which can be found in this chapter.

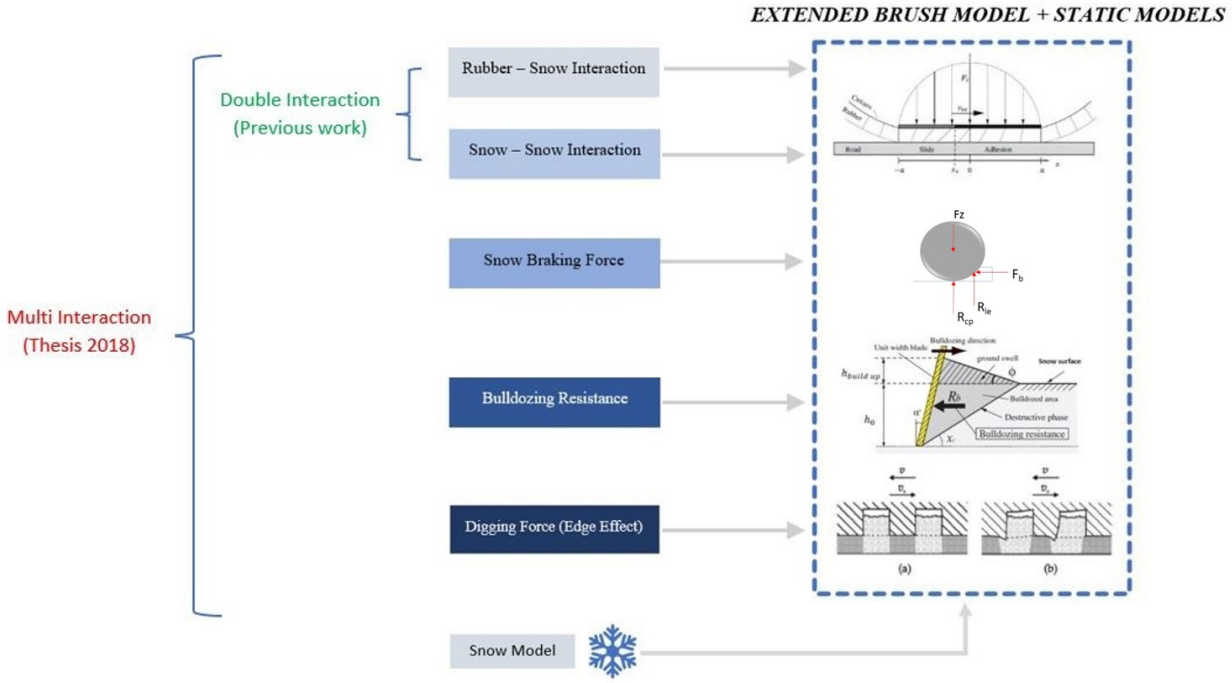

6.1 Multi Interaction Model

6.1.1 Longitudinal Slip Curve

The results for the Nordic and European Tires are show below. It is assumed that the test was carried out in snow, which can be considered as hard packed snow. Thus all calculations pertaining to the results are with respect to D7 snow.

The results that are plotted show both a braking case and a traction case. Although the test results for a traction case is unavailable, it is expected to deliver a result as shown.

The figure 6.1 represents how the different forces act during the braking and traction case. Also, the sign of F_b changes depending on the case.

$$Fx_{(Braking)} = F_{x-rs} + F_{x-ss} + F_b + F_D \tag{6.1}$$

$$Fx_{(Traction)} = F_{x-rs} + F_{x-ss} - F_b + F_D \tag{6.2}$$

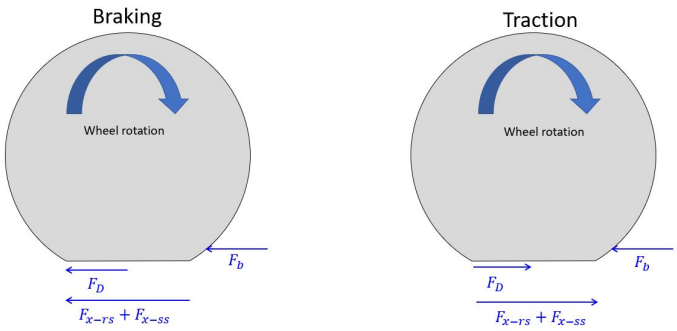

Figure 6.1: Illustration of force combination (longitudinal)

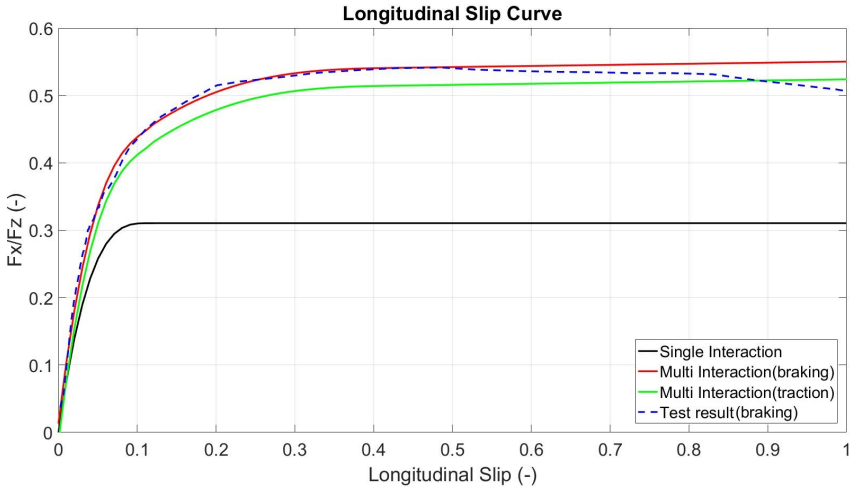

Figure 6.2: Longitudinal Slip Curve (Nordic Tire)

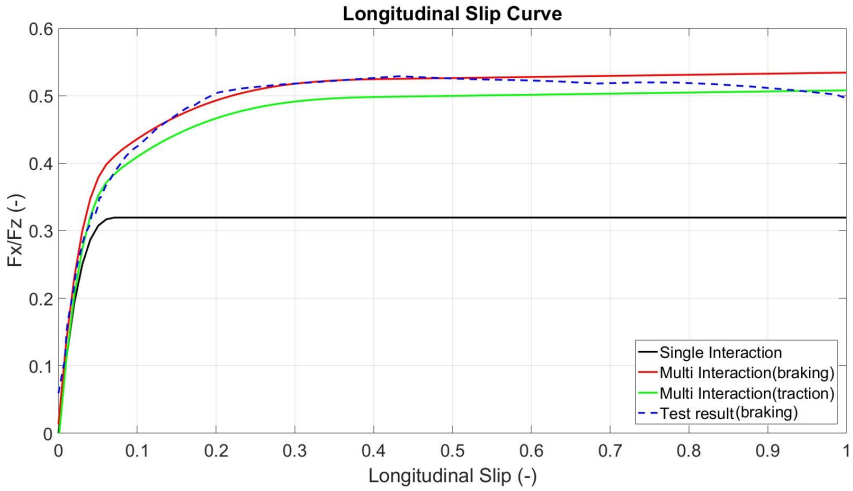

Figure 6.3: Longitudinal Slip Curve (European Tire)

Looking at the results, it can be seen that the single interaction model cannot predict the interaction on snow after a maximum slip of 0.05. The multi interaction model on the other hand predicts the results fairly well, until a slip range of around 0.5.

6.1.2 Lateral Slip Curve

This section shows the forces in the lateral direction. Plotted are the test results, with comparison to the single interaction and multi interaction models.

The irregularities seen in the test results is potentially due to the measurement errors while actuating the mechanism to steer the wheel on the BV12 test rig.
The summing up of forces for the lateral case is given by,

$$Fy_{(Steering)} = F_{y-rs} + F_{y-ss} + F_{br} + F_D \tag{6.3}$$

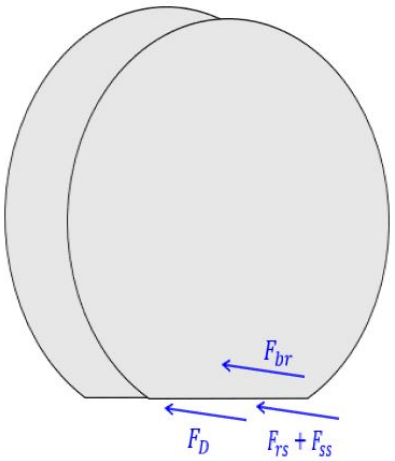

Figure 6.4: Illustration of force combination (lateral)

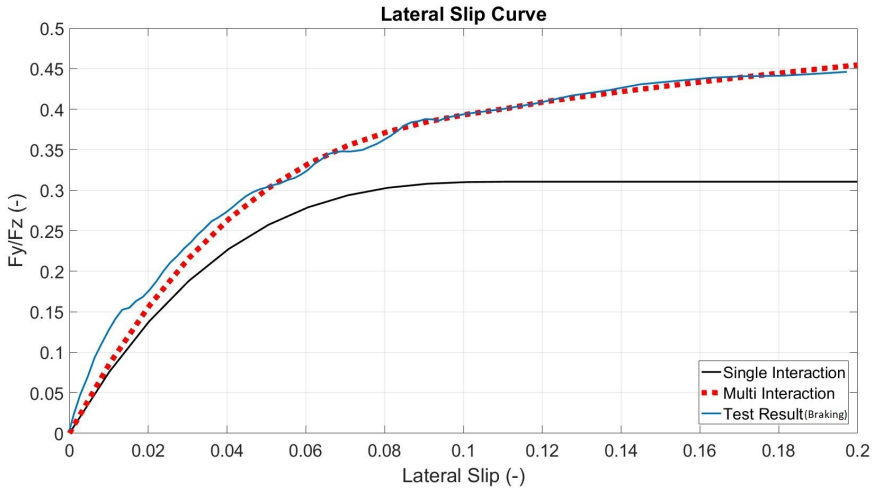

Figure 6.5: Lateral Slip Curve (Nordic Tire)

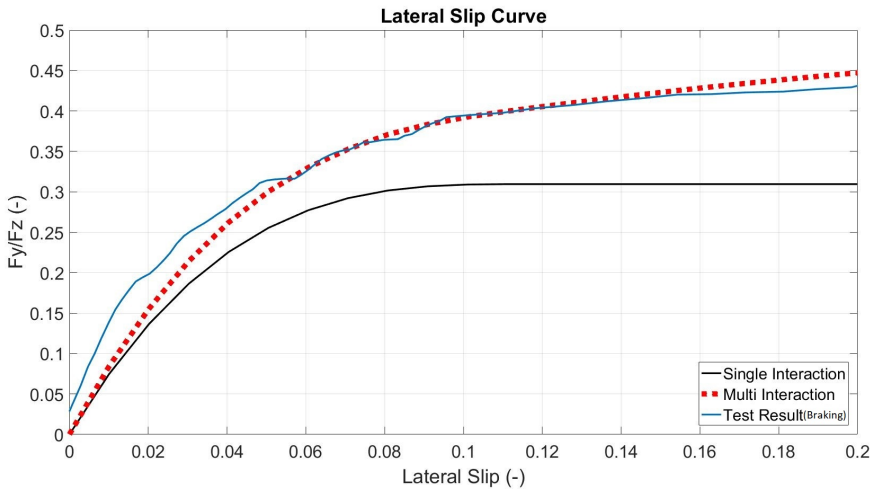

Figure 6.6: Lateral Slip Curve (European Tire)

As can be seen, the results match well with the test results for both the Nordic and European tires. It is important to note that the results available are at small slip ranges and its at this slip range that the model works well.

6.2 Contribution to Force Generation

This section shows the magnitude of the forces that contribute to traction of a tire's interaction on snow. The results shown in the next section are for both the longitudinal and lateral cases and are self explanatory. It is to be noted that our model predicts these fore contribution, but cannot be verified as there are no individual test results available. Further, the magnitudes shown in the figures below show peak force generation in Newtons in accordance to the peak force generated in the longitudinal and lateral slip curves plotted in section 6.1.1.

6.2.1 Force Generation - Nordic Tire

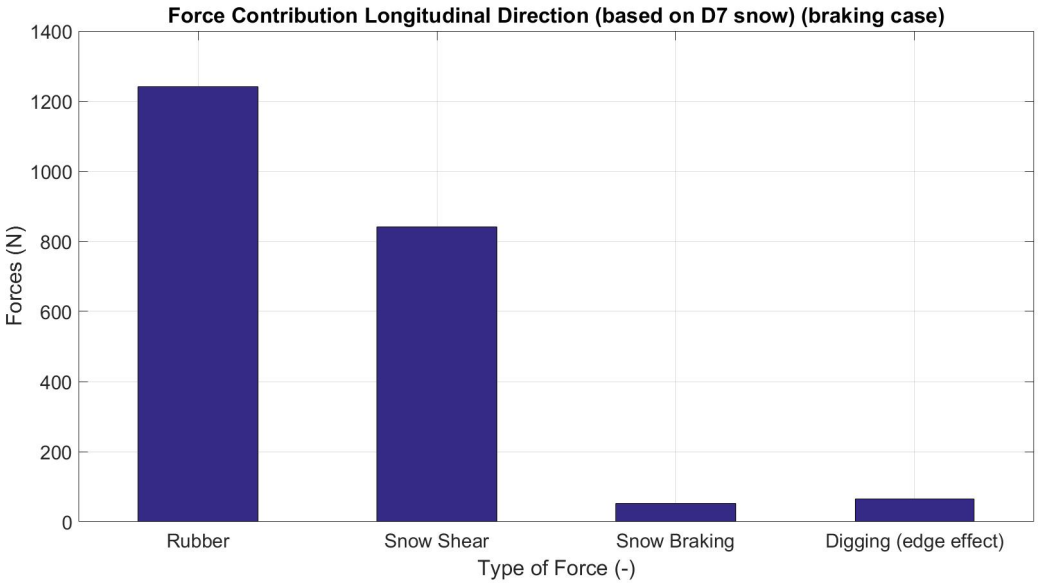

Figure 6.7: Peak Longitudinal Force Contribution for a Braking Case (Nordic Tire)

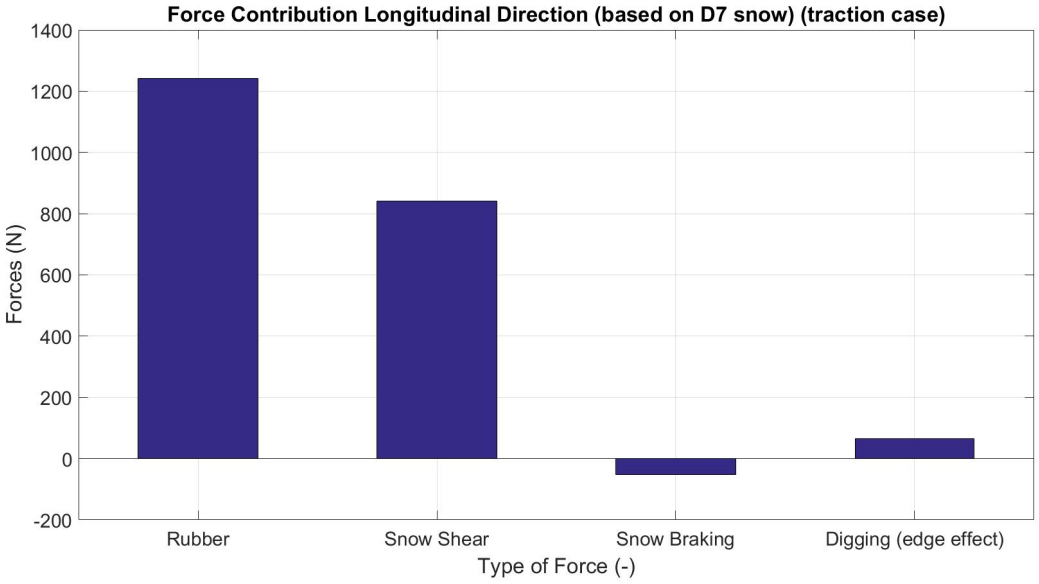

Figure 6.8: Peak Longitudinal Force Contribution for a Traction Case (Nordic Tire)

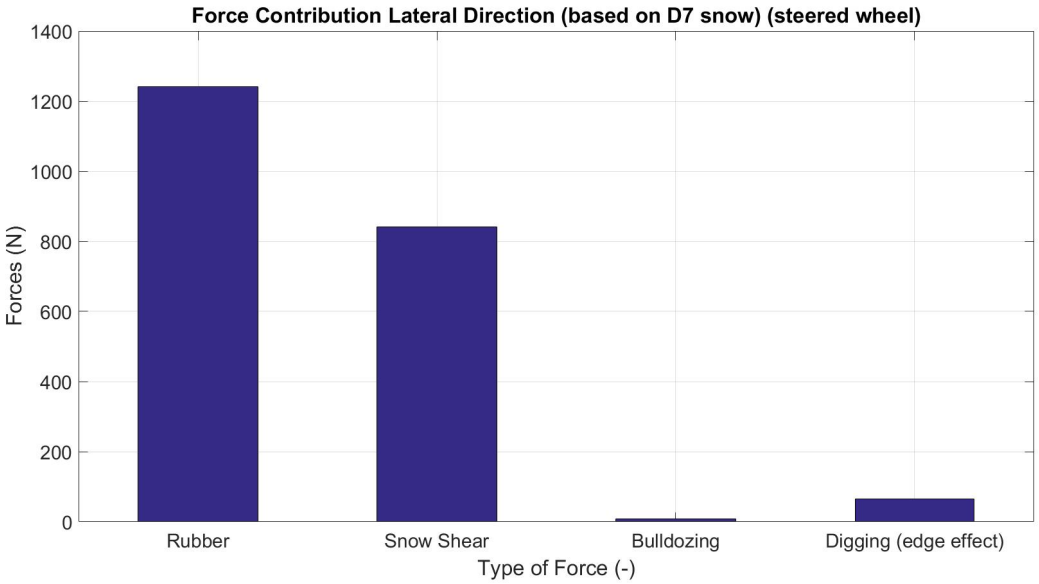

Figure 6.9: Peak Lateral Force Contribution for a Steered Case (Nordic Tire)

6.2.2 Force Generation - European Tire

In this section, the force contribution of a European tire is shown. Comparing it to the Nordic tire, a fairly small but evident difference can be seen. Thus proving that the tire type and design is influencing traction.

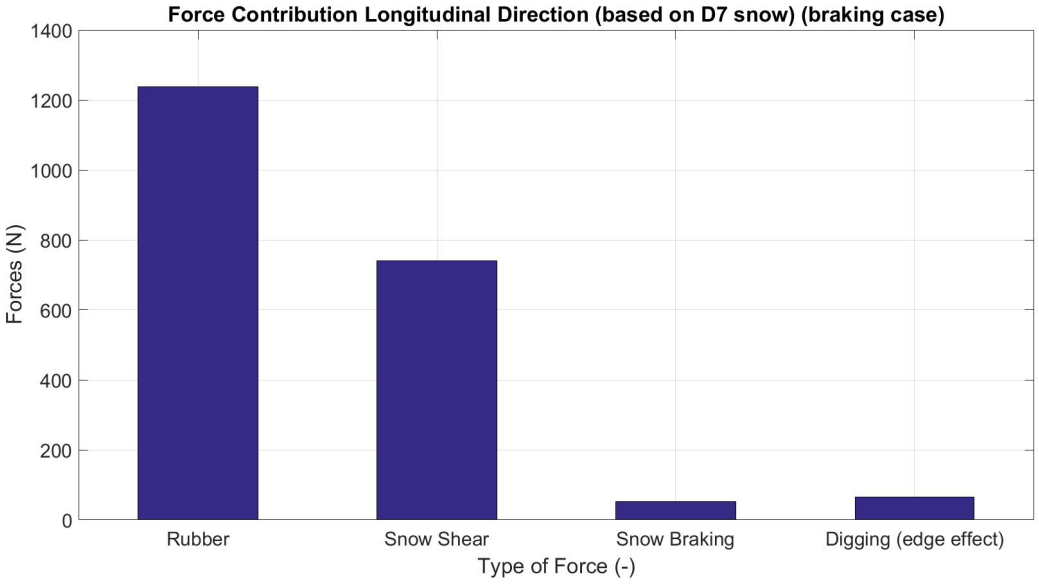

Figure 6.10: Peak Longitudinal Force Contribution for a Braking Case (European Tire)

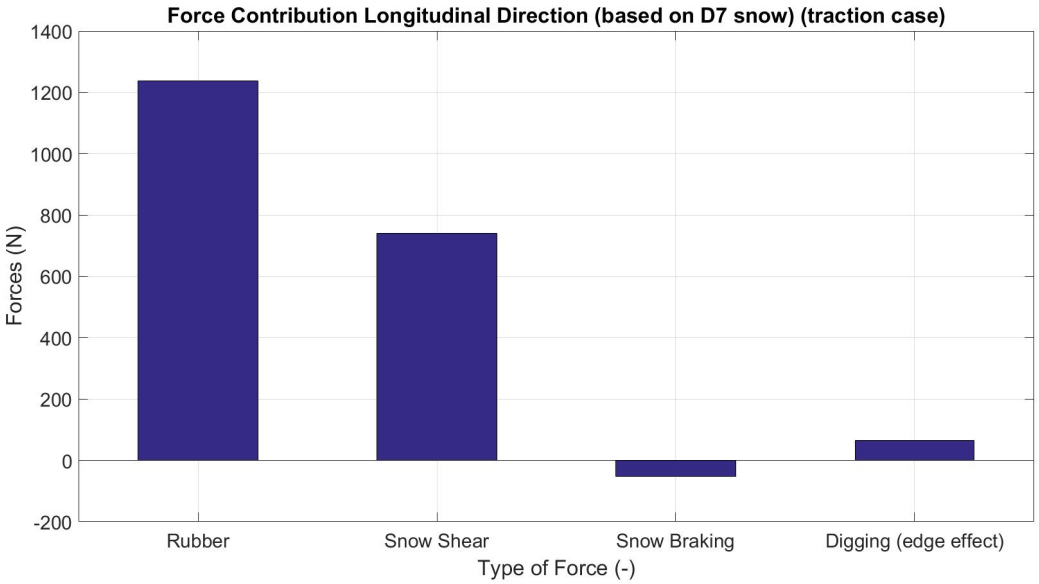

Figure 6.11: Peak Longitudinal Force Contribution for a Traction Case (European Tire)

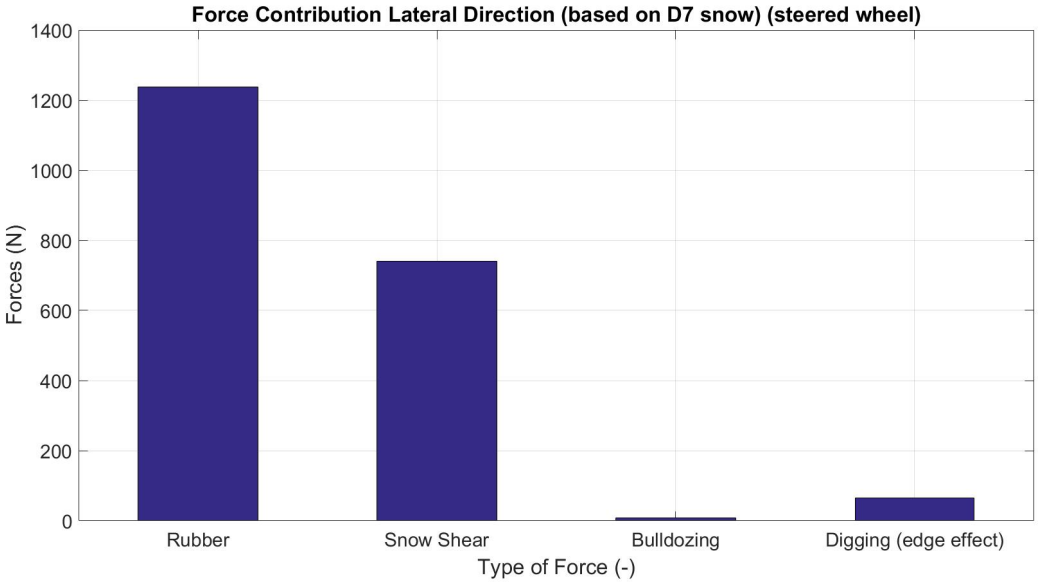

Figure 6.12: Peak Lateral Force Contribution for a Steered Case (European Tire)

6.3 Simulation Results

Simulations using the multi interaction tire model is carried out on a two track model and compared with other models. The two track model considered is a simple model that doesn't account for any load transfer or suspension kinematics, among others. The main focus is to check the effect of the various force contributions and the effect they have during simulations.

6.4 Sine Wave Test

The sine wave test at 50 kmph was tested with three models, double interaction, multi interaction and high-mu model (asphalt). As can be seen from the graph, the difference between the double and multi interaction is visibly small, but could potentially be perceived by a driver in a simulator.

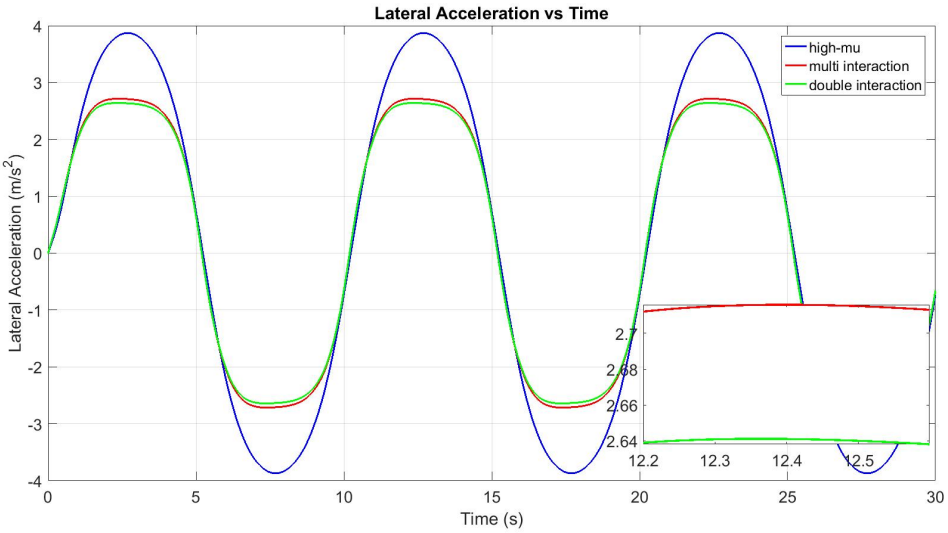

Figure 6.13: Sine Wave Test - Lateral Acceleration

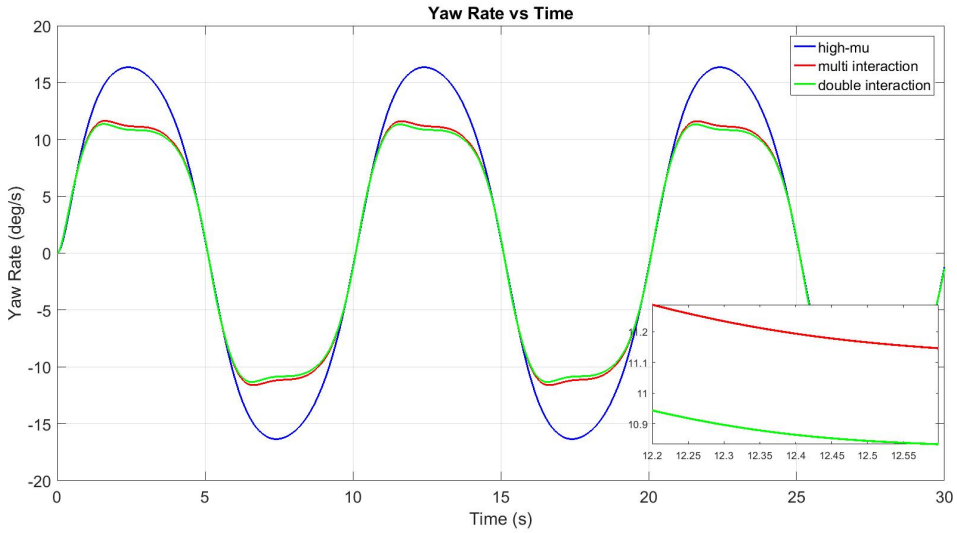

Figure 6.14: Sine Wave Test - Yaw Rate

6.5 Straight Line Braking

The same two track model used for the previous test is used to simulate a straight line braking test. A braking force of 3000N is applied to the axles with a brake bias of 0.5 between the front and rear axles.

To study the effect of the snow and its ability to provide a braking force, snow of 25mm height is assumed to be compressed by the front axles under braking. From the equations used to calculate the snow braking force as discussed in section 5.3, the force is measured and entered into the simulation. The braking force applied by the 'driver' is maintained at 0.5 slip range through out the simulation, thus operating close to its peak friction. Figure 6.15 shows the results of this simulation.

These results are important for validating braking distance on different types of snow surfaces, especially during simulations and for function development.

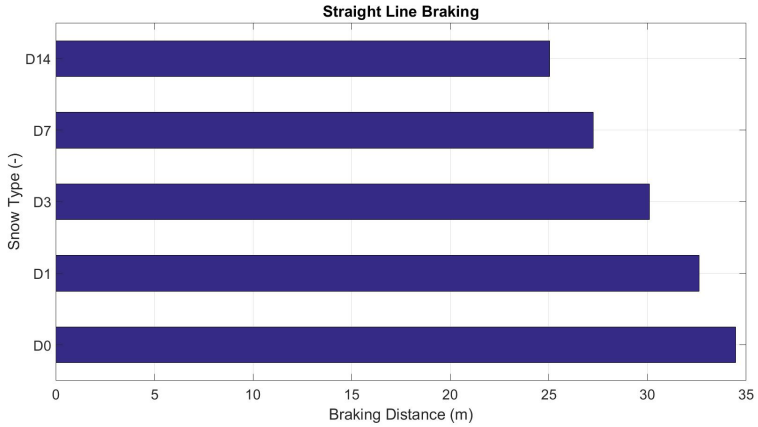

Figure 6.15: Straight Line Braking Test

6.6 Connecting Design Parameters to Performance

An attempt is made to connect tire tread design to performance. Our model predicts that by increasing the void area of a tire ,the braking force reduces. This is because there is much lesser penetration offered from the tread blocks. This might not be an ideal design for a tire running on for instance, ice. But it is ascertained that tire treads can be analytically evaluated.

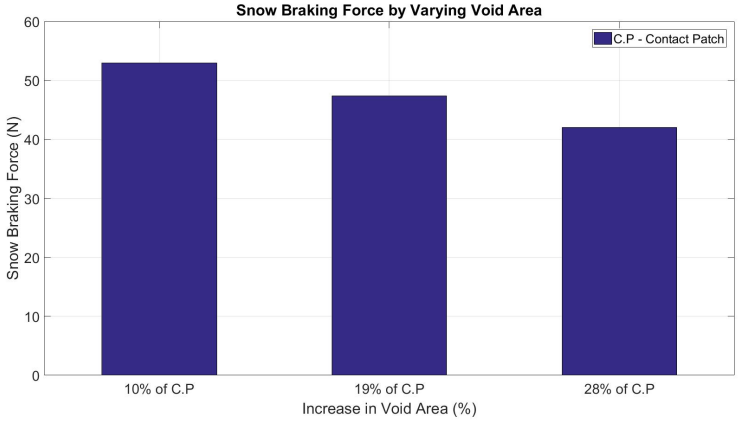

Figure 6.16: Varying Void Ratios

7 Discussion

This thesis extended an already existing model that took into account the snow shear, that is the interaction of snow filled in the tire voids and the snow surface.

To understand the force generation better on a snow surface and hence maximize traction, the overall effect of the forces both in the longitudinal and lateral was established. Though smaller than the rubber - snow and snow - snow interaction, it was important to incorporate the overall effect of the other forces to understand the interaction better.

This thesis work that extended the double interaction model, incorporated the snow braking force into the model. Additionally, the digging force (edge effect) and the bulldozing resistance was evaluated on various snow types. To understand the influence of the added forces viz. snow braking force, digging force and bulldozing resistance, simulations were carried out for both longitudinal and lateral direction. Though the influence is small with these forces incorporated, it is to be noted that the results shown are for a case of D7 snow, that can be ascertained to hard packed snow (due to available test data recorded under these conditions). On such a hard snow type, the penetration is lower and results thus are smaller. Having simulation results on softer snow type could show much larger difference, between incorporating and not incorporating these other forces.

The snow properties considered are necessary to establish accurate models. However, the results that are currently available are far from the real world scenario, as snow is sensitive to temperature, frictional heating and mechanical loading, which have not been considered in the model or in the snow tests. With the properties of snow constantly changing with the number of vehicle passes on snowy roads, it is important to establish better results with respect to snow tests.

Additionally, it is important to address the phenomena of 'ploughing' and 'milling' that has been spoken about in papers [22] and [21], respectively. Many experiments have been conducted to evaluate these forces, which are believed to aid traction. From the results shown in their papers and from the authors view, these terms are an alternative to what happens during digging action of the sipe edges. This effect has been modelled in phase 2 of the digging force as discussed in section 5.5 and is understood to be the same. More information on this phenomena can be found in the papers [22] and [21], and hasn't been explained in this report.

8 Conclusion

From the results of the longitudinal slip curve, it can be seen that the model matches the test results until a slip range of 0.5 and almost accurately in the lateral direction, for the steering sweep range considered. The difference in results in the high slip range for the longitudinal slip curve, can be due to the complex nature of snow and the way it behaves under load and varied ambient conditions. Also, a simple Coulomb friction model was used and having a more advanced friction model that includes Dahl and Stribecks effect, can potentially give a more representative result for the friction phenomena at high slips. The model also does not account for tread patterns on the tire, which can also be a reason for the varied results.

Comparing to the previous work done on this topic, the double interaction model did not include all the plausible forces when a tire is interacting with snow. Though it gives good results in matching the force-slip curves, it is still far from addressing the true phenomena as it doesn't consider snow as a material and the penetration of the tire into the snow. Whereas, the multi interaction model considers all the plausible force interactions and gives the possibility of including the snow properties on which the tire's interaction with. From a parameter level point of view, the double interaction model has few parameters that could be easily varied for each type of tire when compared to a multi interaction model. When the model fidelity is considered, the multi interaction model would justify the fidelity as it takes into account all the forces of tire's interaction on snow and gives a complete physical interpretations of the phenomena. Also, when full vehicle simulations such as for a straight line braking test is performed the multi-interaction model gives a realistic result, as the model has scope to include the snow braking force which is not possible in the double interaction model.

The multi interaction model which takes into account the material properties, can be potentially used for other loose surface such as mud, sand, with the incorporation of their respective material properties. With these statements, the model can be used used to evaluate active safety functions on loose road surfaces.

9 Future Work

A next step is to test the model for different snow types. This though requires real tire test data on different snow types with which it can be evaluated. The brush tire model that has been used can also be further extended by adding the dynamic behaviour of the carcass and also taking into account tire relaxation.

Also, the brush model (elastic bristles and dry friction) used, has been applied to both rubber-snow and snow-snow. Media as snow can be modelled as plastic instead of elastic, which would lead to completely different models, where force is function of sliding speed (m/s) instead of slip (1). To compare these alternative hypotheses one would need tests where braking was done from different vehicle speed.

Though much has not been discussed on aligning torque, the offset of force contribution due to snow shear as seen in figure 5.4 is important to be considered while evaluating aligning torque. Also, the effect of the digging force on aligning torque should be considered, as the force is assumed to arise from the start of the sliding region which will contribute to some moment.

Finally, carrying out scientific research to evaluate the penetration of the sipe edges into the snow layer is important to evaluate the force generation arising out of this digging phenomena.

10 Appendix

In this section, additional plots showing snow braking force for different snow depths are shown.

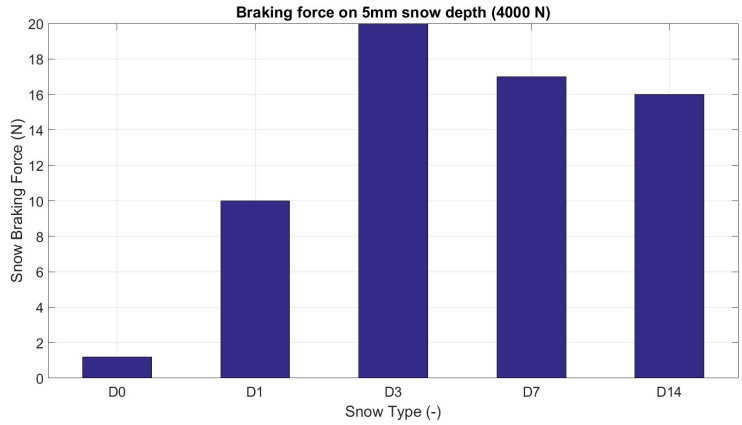

Figure 10.1: Braking Force on 5mm deep snow

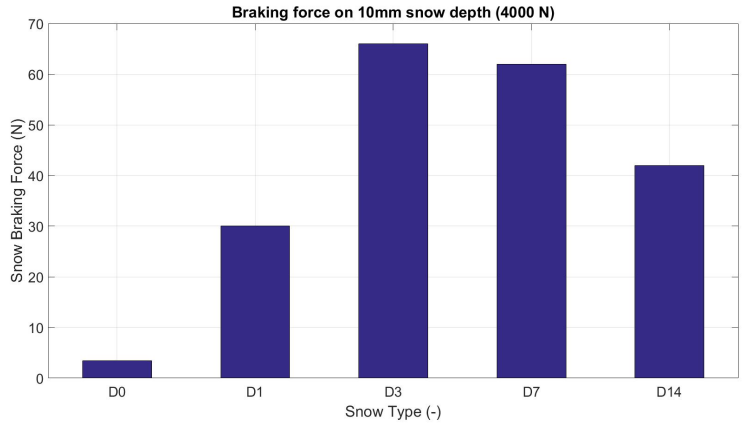

Figure 10.2: Braking Force on 10mm deep snow

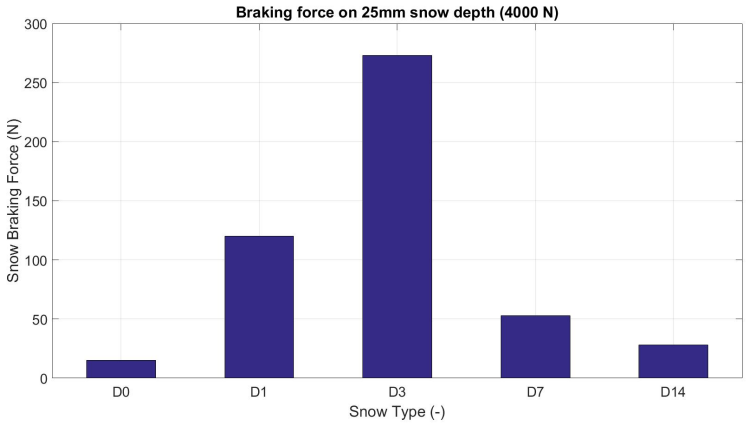

Figure 10.3: Braking Force on 25mm deep snow

10.1 MatLab Code

```
clc; close all; clear all;

%% Initial data

a = 0.160/2;                    % contact patch length of rubber bristle
length = 100-length;
zero_length = round((100 -length));
a_s = (0.16-0.0085)/2;          % contact patch length of snow bristle

ci_x_r = 304.2340*2.1;          % bristle stiffness per unit length()
Cx_r = 12.6121 ;                % stiffness of bristle (longitudinal)
ci_y_r = 238.7890*3.2;          % bristle stiffness per unit length ()
Cy_r = 8.1077;                  % stiffness of bristle (lateral)

ci_x_s = 42.5634*3.9;           % bristle stiffness per unit length ()
Cx_s = 1.292076;                % stiffness of "snow" bristle (longitudinal)
ci_y_s = 25.5208*2.8;           % bristle stiffness per unit length ()
Cy_s = 0.9697;                  % stiffness of "snow" bristle (lateral)

slipX = linspace(0,1,100);      % long. slip
slipY = linspace(0,1,100);      % lat. slip
mu_r2s = 0.30953;               % co-eff. of friction (rubber to snow)
mu_s2s = 0.1852;                % co-eff. of friction (snow to snow)
Fz = 4;                         % normal load (KN)

slipX_s = linspace(0,1,(100-zero_length));
slipY_s = linspace(0,1,(100-zero_length));

%% Matrix coversion AND slip calculations %%

if size(slipX,1)<size(slipX,2)
    slipX = slipX';
end
if size(slipY,1)<size(slipY,2)
    slipY = slipY';
end

if size(slipX_s,1)<size(slipX_s,2)
    slipX_s = slipX_s';
end
if size(slipY_s,1)<size(slipY_s,2)
    slipY_s = slipY_s';
end

cos_beta = -sign(slipX);
sin_beta = -sign(slipY);

cos_beta_s = -sign(slipX_s);
sin_beta_s = -sign(slipY_s);

%Rubber

slipX_lim_r = 3*mu_r2s/(Cx_r);
slipY_lim_r = 3*mu_r2s/(Cy_r);
psiX_r = abs(slipX/slipX_lim_r);
psiY_r = abs(slipY/slipY_lim_r);

%Snow 1
slipX_lim_s = 3*mu_s2s/(Cx_s);
slipY_lim_s = 3*mu_s2s/(Cy_s);
psiX_s = abs(slipX_s/slipX_lim_s);
psiY_s = abs(slipY/slipY_lim_s);

%% Adhesive Forces

Fax_r = Fz*Cx_r*slipX.*(1-psiX_r).^2;
```

```
Fay_r = Fz*Cy_r*slipY.*(1-psiY_r).^2;
Fsx_r = -cos_beta*mu_r2s*Fz.*psiX_r.^2.*(3-2*psiX_r);
Fsy_r = -sin_beta*mu_r2s*Fz.*psiY_r.^2.*(3-2*psiY_r);

%% Sliding Forces

Fax_s = Fz*Cx_s*slipX_s.*(1-psiX_s).^2;
Fay_s = Fz*Cy_s*slipY.*(1-psiY_s).^2;
Fsx_s = -cos_beta_s*mu_s2s*Fz.*psiX_s.^2.*(3-2*psiX_s);
Fsy_s = -sin_beta_s*mu_s2s*Fz.*psiY_s.^2.*(3-2*psiY_s);


%% Time Calculations for "snow" tire formation %%

depth = 8.5/10; % depth of tread (cm)
width = 5/10; % width of void (cm)
breadth = 175/10; % breadth of contact patch (cm)
rho = 0.000397; % Kg/m^3 to N/cm^3(0.48g/cm^3)
rho_a = 1.225; % Kg/cm^3 to N/cm^3
area = breadth*width; % cm^2
vol = depth * area; % cm^3
mass = rho * vol; % N
a = (0.16)*100; % contact patch lemgth (m to cm)
speed = 8.33*100; % wheel speed (cm/s) (30 kmph test as per Artem's paper )

% void fill & mass flow %%

density_conv = rho / 1e-3;                          % converting from kg/cm^3 to kg/l
flow_rate = (area * rho * speed)*60/density_conv;   % l/min % mass flow rate
time_fill = (vol/1000) * (1/flow_rate)*60           % seconds

% bristle %

t_bristle = (a/ speed);                             % entry and exit of bristle in contact patch

percentage_diff = (time_fill./t_bristle)*100 ;      % percentage of time translated to x- direction

perc_diff_dis =  percentage_diff/100 * a

dist_to_form_bris = speed * (time_fill)/100;

length = dist_to_form_bris;

%% Snow braking force %%

%% Tyre specs based on 205/60 R16 tyre %

% switch %

load = 3;

if load == 1
    Fz = 1000/9.81; %(N to kg)
elseif load == 2
    Fz = 2000/9.81; %(N to kg)
else load == 3
    Fz = 4000/9.81; %(N to kg)
end

%% Normal force (Kg) % 1000, 2000, 4000

void_case = 4;      % 1. 0.5cm
                    % 2. 1cm
                    % 3. 2cm
                    % 4. 2.5cm
                    % 5. 3cm
                    % 6. 4cm

snow = 5;           % 1:D0
                    % 2:D1
                    % 3:D3
```

```
                    % 4:D7
                    % 5:D14

alpha = 10/10;         % width of void(mm to cm) % contact length relative to void surface
b = (205-40)/10;      % contact width (mm to cm) - width in contact (approximated) from figure and data as in BOX
L = 160/10;           % length of contact patch (mm to cm)
rvc = (alpha*b*3)/((L*b)); % ratio of void area and contact area (void area + actual contact area)

z = (643/2)/10;          % loaded radius (m to cm)
R = (653/2)/10;          % free rolling radius (m to cm)

%% Snow selection and contatc length of tire surface %%

if void_case == 1 % 0.5 cm depth from surface

H = 8.5/10;             % height of void (mm to cm)
phi = 0.005;            % contact angle (rad)
l = R*phi/10;           % leading edge arc length (cm)

elseif void_case == 2 % 1 cm depth from surface

H = 8.5/10;             % height of void (mm)
phi = 0.061;            % contact angle (rad)
l = R*phi/10;           % leading edge arc length (cm)

elseif void_case == 3 % 2 cm depth from surface

H = 8.5/10;             % height of void (mm)
phi = 0.151;            % contact angle (rad)
l = R*phi/10;           % leading edge arc length (cm)

elseif void_case == 4 % 25 cm depth from surface

H = 8.5/10;             % height of void (mm)
phi = 0.189            % contact angle (rad)
l = R*phi/10;           % leading edge arc length (cm)

elseif void_case == 5 % 30 cm depth from surface

H = 8.5/10;             % height of void (mm)
phi = 0.224;            % contact angle (rad)
l = R*phi/10;           % leading edge arc length (cm)

elseif void_case == 6 % 4 cm depth from surface

H = 8.5/10;             % height of void (mm)
phi = 0.288;            % contact angle (rad)
l = R*phi/10;           % leading edge arc length (cm)

end

%%

if void_case == 1  % .5cm depth from surface

    if snow == 1
        sigma_h_block = 0.0116;
    elseif snow == 2
        sigma_h_block = 0.0963;
    elseif snow == 3
        sigma_h_block = 0.19885;
    elseif snow == 4
        sigma_h_block = 0.1695;
    else snow == 5
        sigma_h_block = 0.5615;
    end

elseif void_case == 2 % 1cm depth from surface

    if snow == 1
        sigma_h_block = 0.03288;
```

```
        sigma_h_void = 0.012;
        sigma_H = 0.028; % values from graph depending on penetration resistance...
                         % ...difference of void height and snow depth read from graph (see in report - section
    elseif snow == 2
        sigma_h_block = 0.284;
        sigma_h_void = 0.2633;
        sigma_H = 0.2;
    elseif snow == 3
        sigma_h_block = 0.633;
        sigma_h_void = 0.49;
        sigma_H = 0.2;
    elseif snow == 4
        sigma_h_block = 0.7455;
        sigma_h_void = 0.2106;
        sigma_H = 0.4;
    else snow == 5
        sigma_h_block = 1.5279;
        sigma_h_void = 2.067;
        sigma_H = 1.1;
    end

elseif void_case == 3   % 2cm depth from surface

    if snow == 1
        sigma_h_block = 0.09604;
        sigma_h_void = 0.04044;
        sigma_H = 0.08;
    elseif snow == 2
        sigma_h_block = 0.8207;
        sigma_h_void = 0.3545;
        sigma_H = 0.55;
    elseif snow == 3
        sigma_h_block = 1.8808;
        sigma_h_void = 0.78175;
        sigma_H = 1.15;
    elseif snow == 4
        sigma_h_block = 3.083;
        sigma_h_void = 1.01075;
        sigma_H = 2.35;
    else snow == 5
        sigma_h_block = 4.2981;
        sigma_h_void = 1.8939;
        sigma_H = 2.65;
    end


elseif void_case == 4   % 2.5cm depth from surface

    if snow == 1
        sigma_h_block = 0.1393;
        sigma_h_void = 0.06981;
        sigma_H = 0.076;
    elseif snow == 2
        sigma_h_block = 1.0961;
        sigma_h_void = 0.62615;
        sigma_H = 0.537;
    elseif snow == 3
        sigma_h_block = 2.4838;
        sigma_h_void = 1.42005;
        sigma_H = 1.281;
    elseif snow == 4
        sigma_h_block = 4.19215;
        sigma_h_void = 2.2375;
        sigma_H = 2.39;
    else snow == 5
        sigma_h_block = 5.5223;
        sigma_h_void = 3.34895;
        sigma_H = 2.69;
    end
```

```
elseif void_case == 5   % 3cm depth from surface

    if snow == 1
        sigma_h_block = 0.09604;
        sigma_h_void = 0.04044;
        sigma_H = 0.090;
    elseif snow == 2
        sigma_h_block = 0.8207;
        sigma_h_void = 0.3545;
        sigma_H = 0.59;
    elseif snow == 3
        sigma_h_block = 1.8808;
        sigma_h_void = 0.78175;
        sigma_H = 1.34;
    elseif snow == 4
        sigma_h_block = 3.083;
        sigma_h_void = 1.01075;
        sigma_H = 2.47;
    else snow == 5
        sigma_h_block = 4.2981;
        sigma_h_void = 1.8939;
        sigma_H = 2.73;
    end
else void_case == 6   % 4cm depth from surface

    if snow == 1
        sigma_h_block = 0.28587;
        sigma_h_void = 0.230;
        sigma_H = 0.09;
    elseif snow == 2
        sigma_h_block = 2.3049;
        sigma_h_void = 1.57;
        sigma_H = 0.77;
    elseif snow == 3
        sigma_h_block = 4.525;
        sigma_h_void = 3.364;
        sigma_H = 1.36;
    elseif snow == 4
        sigma_h_block = 8.0935;
        sigma_h_void = 5.846;
        sigma_H = 2.64;
    else snow == 5
        sigma_h_block = 9.689;
        sigma_h_void = 7.3124;
        sigma_H = 2.80;
    end
end

%%  stress in z- direction %%
if void_case == 1

    sigma_z_b = (sigma_h_block/(l))*cosd(45);

    syms sigma_ho
    eq31 = Fz == (L*b*sigma_ho*(1-rvc)) + (b*l*(1-rvc)*sigma_z_b)
    sigma_ho_1 = double(solve(eq31,sigma_ho))

elseif void_case == 2

    sigma_z_b = (sigma_h_block/(l))*cosd(45);
    sigma_z_v = (sigma_h_void/(alpha))*cosd(45);

    syms sigma_ho
    eq32 = Fz == (L*b*(sigma_ho*(1-rvc)) + (sigma_ho - sigma_H)* rvc)+ b*l*(1-rvc)*sigma_z_b+...
        b*alpha*rvc*sigma_z_v;
    sigma_ho_2 = double(solve(eq32,sigma_ho))

elseif void_case == 3

    sigma_z_b = (sigma_h_block/l)*cosd(45);
    sigma_z_v = (sigma_h_void/alpha)*cosd(45);
```

```
    syms sigma_ho
   eq33 = Fz == (L*b*(sigma_ho*(1-rvc)) + (sigma_ho - sigma_H)* rvc)+ b*l*(1-rvc)*sigma_z_b+...
        b*alpha*rvc*sigma_z_v;
    sigma_ho_2 = double(solve(eq33,sigma_ho))

    else void_case == 4

    sigma_z_b = (sigma_h_block/l)*cosd(45);
    sigma_z_v = (sigma_h_void/alpha)*cosd(45);

    syms sigma_ho
    eq34 = Fz == (L*b*(sigma_ho*(1-rvc)) + (sigma_ho - sigma_H)* rvc)+ b*l*(1-rvc)*sigma_z_b+...
        b*alpha*rvc*sigma_z_v;
    sigma_ho_2 = double(solve(eq34,sigma_ho))

end

%% interpolate for each value of sigma_ho to find h0 for various snow depths and type of snow %%
%% done from graph as seen in snow test section in report %%
%% stress in x - direction %%

if void_case == 1 && load == 1

    if snow == 1
        h0 = 0.5;
        sigma_h_penetration_block = 0.0116;
    elseif  snow == 2
        h0 = 0.43;
        sigma_h_penetration_block = 0.059;
    elseif  snow == 3
        h0 = 0.22;
        sigma_h_penetration_block = 0.042;
    elseif  snow == 4
        h0 = 0.25;
        sigma_h_penetration_block = 0.03;
    else snow == 5
        h0 = 0;
        sigma_h_penetration_block = 0;
    end

elseif void_case == 1 && load == 2

    if snow == 1
        h0 = 0.5;
        sigma_h_penetration_block = 0.0116;
    elseif  snow == 2
        h0 = 0.5;
        sigma_h_penetration_block = 0.0963;
    elseif  snow == 3
        h0 = 0.5;
        sigma_h_penetration_block = 0.19885;
    elseif  snow == 4
        h0 = 0.5;
        sigma_h_penetration_block = 0.1695;
    else snow == 5
        h0 = 0;
        sigma_h_penetration_block = 0;
    end

elseif void_case == 1 && load == 3

    if snow == 1
        h0 = 0.5;
        sigma_h_penetration_block = 0.0116;
    elseif  snow == 2
        h0 = 0.5;
        sigma_h_penetration_block = 0.0963;
    elseif  snow == 3
        h0 = 0.5;
        sigma_h_penetration_block = 0.199;
```

```
    elseif  snow == 4
        h0 = 0.5;
        sigma_h_penetration_block = 0.1695;
    else snow == 5
        h0 = 0.45;
        sigma_h_penetration_block = 0.1585;
    end

elseif void_case == 2 && load == 1

    if snow == 1
        h0 = 1;
        sigma_h_penetration_block = 0.0329;
        sigma_h_penetration_void = .012;
    elseif  snow == 2
        h0 = 0.45;
        sigma_h_penetration_block = 0.06;
        sigma_h_penetration_void = 0;
    elseif  snow == 3
        h0 = 0.23;
        sigma_h_penetration_block = 0.041;
        sigma_h_penetration_void = 0;
    elseif  snow == 4
        h0 = 0.28;
        sigma_h_penetration_block = 0.033;
        sigma_h_penetration_void = 0;
    else snow == 5
        h0 = 0;
        sigma_h_penetration_block = 0;
        sigma_h_penetration_void = 0;
    end

elseif void_case == 2 && load == 2

    if snow == 1
        h0 = 1;
        sigma_h_penetration_block = 0.0329;
        sigma_h_penetration_void = 0.003;
    elseif  snow == 2
        h0 = 1;
        sigma_h_penetration_block = 0.284;
        sigma_h_penetration_void = 0.02;
    elseif  snow == 3
        h0 = 0.56;
        sigma_h_penetration_block = 0.31;
        sigma_h_penetration_void = 0;
    elseif  snow == 4
        h0 = 0.48;
        sigma_h_penetration_block = 0.165;
        sigma_h_penetration_void = 0;
    else snow == 5
        h0 = 0;
        sigma_h_penetration_block = 0;
        sigma_h_penetration_void = 0;
    end

elseif void_case == 2 && load == 3

    if snow == 1
        h0 = 1;
        sigma_h_penetration_block = 0.0328;
        sigma_h_penetration_void = 0.003;
    elseif  snow == 2
        h0 = 1;
        sigma_h_penetration_block = 0.284;
        sigma_h_penetration_void = 0.02;
    elseif  snow == 3
        h0 = 1;
        sigma_h_penetration_block = 0.633;
        sigma_h_penetration_void = 0.04;
    elseif  snow == 4
```

```
        h0 = 0.93;
        sigma_h_penetration_block = 0.595;
        sigma_h_penetration_void = 0.013;
    else snow == 5
        h0 = 0.38;
        sigma_h_penetration_block = 0.41;
        sigma_h_penetration_void = 0;
    end

elseif void_case == 3 && load == 1 % 20mm snow

    if snow == 1
        h0 = 2;
        sigma_h_penetration_block = 0.091;
        sigma_h_penetration_void = 0.0404;
    elseif  snow == 2
        h0 = 0.38;
        sigma_h_penetration_block = 0.05755;
        sigma_h_penetration_void = 0;
    elseif  snow == 3
        h0 = 0.16;
        sigma_h_penetration_block = 0.027;
        sigma_h_penetration_void = 0;
    elseif  snow == 4
        h0 = 0.13;
        sigma_h_penetration_block = 0.012;
        sigma_h_penetration_void = 0;
    else snow == 5
        h0 = 0;
        sigma_h_penetration_block = 0;
        sigma_h_penetration_void = 0;
    end

elseif void_case == 3 && load == 2

    if snow == 1
        h0 = 2;
        sigma_h_penetration_block = 0.091;
        sigma_h_penetration_void = 0.0404;
    elseif  snow == 2
        h0 = 2;
        sigma_h_penetration_block = 0.7919;
        sigma_h_penetration_void = 0.3545;
    elseif  snow == 3
        h0 = 0.43;
        sigma_h_penetration_block = 0.14;
        sigma_h_penetration_void = 0;
    elseif  snow == 4
        h0 = 0.41;
        sigma_h_penetration_block = 0.108;
        sigma_h_penetration_void = 0;
    else snow == 5
        h0 = 0;
        sigma_h_penetration_block = 0;
        sigma_h_penetration_void = 0;
    end

elseif void_case == 3 && load == 3

    if snow == 1
        h0 = 2;
        sigma_h_penetration_block = 0.091;
        sigma_h_penetration_void = 0.0404;
    elseif  snow == 2
        h0 = 2;
        sigma_h_penetration_block = 0.7919;
        sigma_h_penetration_void = 0.3545;
    elseif  snow == 3
        h0 = 2;
        sigma_h_penetration_block = 1.8808;
        sigma_h_penetration_void = 0.781;
```

```
    elseif  snow == 4
        h0 = 0.86;
        sigma_h_penetration_block = 0.525;
        sigma_h_penetration_void = 0;
    else snow == 5
        h0 = 0.31;
        sigma_h_penetration_block = 0.0629;
        sigma_h_penetration_void = 0;
    end

    elseif void_case == 4 && load == 1 %2.5cm

    if snow == 1
        h0 = 2.5;
        sigma_h_penetration_block = 0.1393;
        sigma_h_penetration_void = 0.06981;
    elseif  snow == 2
        h0 = 0.38;
        sigma_h_penetration_block = 0.05755;
        sigma_h_penetration_void = 0;
    elseif  snow == 3
        h0 = 0.15;
        sigma_h_penetration_block = 0.011;
        sigma_h_penetration_void = 0;
    elseif  snow == 4
        h0 = 0.08;
        sigma_h_penetration_block = 0.006;
        sigma_h_penetration_void = 0;
    else snow == 5
        h0 = 0;
        sigma_h_penetration_block = 0;
        sigma_h_penetration_void = 0;
    end

elseif void_case == 4 && load == 2

    if snow == 1
        h0 = 2.5;
        sigma_h_penetration_block = 0.1393;
        sigma_h_penetration_void = 0.06981;
    elseif  snow == 2
        h0 = 2.5;
        sigma_h_penetration_block = 1.0961;
        sigma_h_penetration_void = 0.62615;
    elseif  snow == 3
        h0 = 0.41;
        sigma_h_penetration_block = 0.1276;
        sigma_h_penetration_void = 0;
    elseif  snow == 4
        h0 = 0.36;
        sigma_h_penetration_block = 0.08;
        sigma_h_penetration_void = 0;
    else snow == 5
        h0 = 0;
        sigma_h_penetration_block = 0;
        sigma_h_penetration_void = 0;
    end

elseif void_case == 4 && load == 3

    if snow == 1
        h0 = 2.5;
        sigma_h_penetration_block = 0.1393;
        sigma_h_penetration_void = 0.06981;
    elseif  snow == 2
        h0 = 2.5;
        sigma_h_penetration_block = 1.0961;
        sigma_h_penetration_void = 0.62615;
    elseif  snow == 3
        h0 = 2.5;
        sigma_h_penetration_block = 2.4838;
```

```
        sigma_h_penetration_void = 1.42005;
    elseif  snow == 4
        h0 = 0.84;
        sigma_h_penetration_block = 0.51;
        sigma_h_penetration_void = 0;
    else snow == 5
        h0 = 0.285;
        sigma_h_penetration_block = 0.2755;
        sigma_h_penetration_void = 0;
    end
    elseif void_case == 5 && load == 1 % 3 cm depth of snow

    if snow == 1
        h0 = 3;
        sigma_h_penetration_block = 0.188;
        sigma_h_penetration_void = 0.110015;
    elseif  snow == 2
        h0 = 0.38;
        sigma_h_penetration_block = 0.05755;
        sigma_h_penetration_void = 0;
    elseif  snow == 3
        h0 = 0.13;
        sigma_h_penetration_block = 0.010;
        sigma_h_penetration_void = 0;
    elseif  snow == 4
        h0 = 0.18;
        sigma_h_penetration_block = 0.015;
        sigma_h_penetration_void = 0;
    else snow == 5
        h0 = 0;
        sigma_h_penetration_block = 0;
        sigma_h_penetration_void = 0;
    end

elseif void_case == 5 && load == 2

    if snow == 1
        h0 = 3;
        sigma_h_penetration_block = 0.188;
        sigma_h_penetration_void = 0.110015;
    elseif  snow == 2
        h0 = 3;
        sigma_h_penetration_block = 1.43825;
        sigma_h_penetration_void = 0.910;
    elseif  snow == 3
        h0 = 0.43;
        sigma_h_penetration_block = 0.14;
        sigma_h_penetration_void = 0;
    elseif  snow == 4
        h0 = 0.41;
        sigma_h_penetration_block = 0.108;
        sigma_h_penetration_void = 0;
    else snow == 5
        h0 = 0;
        sigma_h_penetration_block = 0;
        sigma_h_penetration_void = 0;
    end

elseif void_case == 5 && load == 3

    if snow == 1
        h0 = 3;
        sigma_h_penetration_block = 0.188;
        sigma_h_penetration_void = 0.110015;
    elseif  snow == 2
        h0 = 3;
        sigma_h_penetration_block = 1.43825;
        sigma_h_penetration_void = 0.910;
    elseif  snow == 3
        h0 = 3;
        sigma_h_penetration_block = 3.160;
```

```
        sigma_h_penetration_void = 2.080;
    elseif  snow == 4
        h0 = 0.86;
        sigma_h_penetration_block = 0.48;
        sigma_h_penetration_void = 0;
    else snow == 5
        h0 = 0.31;
        sigma_h_penetration_block = 0.275;
        sigma_h_penetration_void = 0;
    end

elseif void_case == 6 && load == 1 % 4cm depth

    if snow == 1
        h0 = 4;
        sigma_h_penetration_block = 0.2858;
        sigma_h_penetration_void = 0.201;
    elseif  snow == 2
        h0 = 0.28;
        sigma_h_penetration_block = 0.028;
        sigma_h_penetration_void = 0;
    elseif  snow == 3
        h0 = 0.13;
        sigma_h_penetration_block = 0.016;
        sigma_h_penetration_void = 0;
    elseif  snow == 4
        h0 = 0;
        sigma_h_penetration_block = 0;
        sigma_h_penetration_void = 0;
    else snow == 5
        h0 = 0;
        sigma_h_penetration_block = 0;
        sigma_h_penetration_void = 0;
    end

elseif void_case == 6 && load == 2

    if snow == 1
        h0 = 4;
        sigma_h_penetration_block = 0.2858;
        sigma_h_penetration_void = 0.201;
    elseif  snow == 2
        h0 = 2.9;
        sigma_h_penetration_block = 1.4;
        sigma_h_penetration_void = 0.3545;
    elseif  snow == 3
        h0 = 0.26;
        sigma_h_penetration_block = 0.04;
        sigma_h_penetration_void = 0;
    elseif  snow == 4
        h0 = 0.31;
        sigma_h_penetration_block = 0.0615;
        sigma_h_penetration_void = 0;
    else snow == 5
        h0 = 0;
        sigma_h_penetration_block = 0;
        sigma_h_penetration_void = 0;
    end

elseif void_case == 6 && load == 3

    if snow == 1
        h0 = 4;
        sigma_h_penetration_block = 0.2858;
        sigma_h_penetration_void = 0.201;
    elseif  snow == 2
        h0 = 4;
        sigma_h_penetration_block = 2.3;
        sigma_h_penetration_void = 1.51;
    elseif  snow == 3
        h0 = 4;
```

```
        sigma_h_penetration_block = 4.52;
        sigma_h_penetration_void = 3.36429;
    elseif  snow == 4
        h0 =0.73;
        sigma_h_penetration_block = 0.37;
        sigma_h_penetration_void = 0;
    else snow == 5
        h0 = 0.18;
        sigma_h_penetration_block = 0.15;
        sigma_h_penetration_void = 0;
    end

end

%% Braking Resistance %%

if void_case == 1

    sigma_b = (sigma_h_penetration_block/h0)*cosd(45);

    Fb = (h0 *b*(1-rvc)*sigma_b)*9.81; % Newton

elseif void_case == 2

    sigma_b = (sigma_h_penetration_block/h0)*cosd(45);
    sigma_v = (sigma_h_penetration_void/(h0-H))*cosd(45);

    Fb = (h0*b*(1-rvc)*sigma_b + (h0-H)*b*rvc*sigma_v)*9.81; % Newton

elseif void_case == 3

    sigma_b = (sigma_h_penetration_block/h0)*cosd(45);
    sigma_v = (sigma_h_penetration_void/(h0-H))*cosd(45);

    Fb = (h0*b*(1-rvc)*sigma_b + (h0-H)*b*rvc*sigma_v)*9.81; % Newton

elseif void_case == 4

    sigma_b = (sigma_h_penetration_block/h0) *cosd(45);
    sigma_v = (sigma_h_penetration_void/(h0-H)) *cosd(45);

    Fb = (h0*b*(1-rvc)*sigma_b + (h0-H)*b*rvc*sigma_v)*9.81; % Newton

elseif void_case == 5

    sigma_b = (sigma_h_penetration_block/h0) *cosd(45);
    sigma_v = (sigma_h_penetration_void/(h0-H)) *cosd(45);

    Fb = (h0*b*(1-rvc)*sigma_b + (h0-H)*b*rvc*sigma_v)*9.81; % Newton

elseif void_case == 6

    sigma_b = (sigma_h_penetration_block/h0) *cosd(45);
    sigma_v = (sigma_h_penetration_void/(h0-H)) *cosd(45);

    Fb = (h0*b*(1-rvc)*sigma_b + (h0-H)*b*rvc*sigma_v)*9.81; % Newton
end

%% Bulldozing resistance %%

void_case = 4; % 1. 0.5cm, 2. 1cm, 3. 2cm, 4. 2.5 cm 5, 3 cm 6, 4 cm
load = 3; % 1. 1KN, 2. 2KN, 3. 4KN
snow = 5; % 1. D0, 2. D1, 3. D3, 4. D7, 5. D14

%% data %%

z =  0.643/2                    ; % unloaded wheel radius (m)
b =  0.175                      ; % width of the wheel (m)
lambda = 1                      ; % wheel sinkage ratio
rho = 480                       ; % Snow density (kg/m^3)(dependent on snow)...
                                  % (D0 - 480; D1 - 520; D3 - 490; D7 - 510; D14 - 520))
```

```
alpha = 0                          ; % camber angle
slipY= tand(linspace(0,12,100))' ; % slip angle (deg)
Fz = 4000                          ; % normal load (N)

%% snow density, cohesion stress, friction angle %%

if snow == 1 % D0
    rho = 0.391e3                       ;%density(kg/m^3)
    c = 438.33                          ;% cohesion stress of the snow (kgf/m2)
    phi = atand(0.418)                  ;% internal friction angle of snow  (deg) (from Terramechanics)
    Xc = 45 - phi/2                     ;% Destructive angle (deg)
elseif snow == 2 % D1
    rho = 0.406e3;
    c = 621.814
    phi = 12.077                        ;% internal friction angle of snow  (deg)
    Xc = 45 - phi/2                     ;% Destructive angle (deg)
elseif snow == 3 % D3
    rho = 0.397e3;
    c = 897.049
    phi = 13.768                        ;% internal friction angle of snow  (deg)
    Xc = 45 - phi/2                     ;% Destructive angle (deg)
elseif snow == 4 % D7
    rho = 0.398e3;
    c = 1763.507
    phi = 19.188                        ;% internal friction angle of snow  (deg)
    Xc = 45 - phi/2                     ;% Destructive angle (deg)
else snow == 5 % D14
    rho = 0.398e3;
    c = 1386.34
    phi = 12.519                        ;% internal friction angle of snow  (deg)
    Xc = 45 - phi/2                     ;% Destructive angle (deg)
end

%% penetration depth from Braking force %%

if void_case == 1 && load == 1
    if snow == 1
        h0 = 0.5;
    elseif  snow == 2
        h0 = 0.43;
    elseif  snow == 3
        h0 = 0.22;
    elseif  snow == 4
        h0 = 0.25;
    else snow == 5
        h0 = 0;
    end
elseif void_case == 1 && load == 2
    if snow == 1
        h0 = 0.5;
    elseif  snow == 2
        h0 = 0.5;
    elseif  snow == 3
        h0 = 0.5;
    elseif  snow == 4
        h0 = 0.5;
    else snow == 5
        h0 = 0;
    end
elseif void_case == 1 && load == 3
    if snow == 1
        h0 = 0.5;
    elseif  snow == 2
        h0 = 0.5;
    elseif  snow == 3
        h0 = 0.5;
    elseif  snow == 4
        h0 = 0.5;
    else snow == 5
        h0 = 0.45;
    end
```

```
elseif void_case == 2 && load == 1
    if snow == 1
        h0 = 1;
    elseif  snow == 2
        h0 = 0.45;
    elseif  snow == 3
        h0 = 0.23;
    elseif  snow == 4
        h0 = 0.28;
    else snow == 5
        h0 = 0;
    end
elseif void_case == 2 && load == 2
    if snow == 1
        h0 = 1;
    elseif  snow == 2
        h0 = 1;
    elseif  snow == 3
        h0 = 0.56;
    elseif  snow == 4
        h0 = 0.48;
    else snow == 5
        h0 = 0;
    end
elseif void_case == 2 && load == 3
    if snow == 1
        h0 = 1;
    elseif  snow == 2
        h0 = 1;
    elseif  snow == 3
        h0 = 1;
    elseif  snow == 4
        h0 = 0.93;
    else snow == 5
        h0 = 0.38;
    end
elseif void_case == 3 && load == 1
    if snow == 1
        h0 = 2;
    elseif  snow == 2
        h0 = 0.38;
    elseif  snow == 3
        h0 = 0.16;
    elseif  snow == 4
        h0 = 0.13;
    else snow == 5
        h0 = 0;
    end
elseif void_case == 3 && load == 2
    if snow == 1
        h0 = 2;
    elseif  snow == 2
        h0 = 2;
    elseif  snow == 3
        h0 = 0.43;
    elseif  snow == 4
        h0 = 0.41;
    else snow == 5
        h0 = 0;
    end
elseif void_case == 3 && load == 3
    if snow == 1
        h0 = 2;
    elseif  snow == 2
        h0 = 2;
    elseif  snow == 3
        h0 = 2;
    elseif  snow == 4
        h0 = 0.86;
    else snow == 5
        h0 = 0.31;
```

```
    end
elseif void_case == 4 && load == 1
    if snow == 1
        h0 = 2.5;
    elseif  snow == 2
        h0 = 0.38;
    elseif  snow == 3
        h0 = 0.15;
    elseif  snow == 4
        h0 = 0.08;
    else snow == 5
        h0 = 0;
    end
elseif void_case == 4 && load == 2
    if snow == 1
        h0 = 2.5;
    elseif  snow == 2
        h0 = 2.5;
    elseif  snow == 3
        h0 = 0.41;
    elseif  snow == 4
        h0 = 0.36;
    else snow == 5
        h0 = 0;
    end
elseif void_case == 4 && load == 3
    if snow == 1
        h0 = 2.5;
    elseif  snow == 2
        h0 = 2.5;
    elseif  snow == 3
        h0 = 2.5;
    elseif  snow == 4
        h0 = 0.84;
    else snow == 5
        h0 = 0.285;
    end
elseif void_case == 5 && load == 1
    if snow == 1
        h0 = 3;
    elseif  snow == 2
        h0 = 0.38;
    elseif  snow == 3
        h0 = 0.13;
    elseif  snow == 4
        h0 = 0.18;
    else snow == 5
        h0 = 0;
    end
elseif void_case == 5 && load == 2
    if snow == 1
        h0 = 3;
    elseif  snow == 2
        h0 = 3;
    elseif  snow == 3
        h0 = 0.43;
    elseif  snow == 4
        h0 = 0.41;
    else snow == 5
        h0 = 0;
    end
elseif void_case == 5 && load == 3
    if snow == 1
        h0 = 3;
    elseif  snow == 2
        h0 = 3;
    elseif  snow == 3
        h0 = 3;
    elseif  snow == 4
        h0 = 0.86;
    else snow = 5
```

```
        h0 = 0.31;
    end
elseif void_case == 6 && load == 1
    if snow == 1
        h0 = 4;
    elseif  snow == 2
        h0 = 0.28;
    elseif  snow == 3
        h0 = 0.13;
    elseif  snow == 4
        h0 = 0;
    else snow == 5
        h0 = 0;
    end
elseif void_case == 6 && load == 2
    if snow == 1
        h0 = 4;
    elseif  snow == 2
        h0 = 2.9;
    elseif  snow == 3
        h0 = 0.26;
    elseif  snow == 4
        h0 = 0.31;
    else snow == 5
        h0 = 0;
    end
elseif void_case == 6 && load == 3
    if snow == 1
        h0 = 4;
    elseif  snow == 2
        h0 = 4;
    elseif  snow == 3
        h0 = 4;
    elseif  snow == 4
        h0 = 0.73;
    else snow == 5
        h0 = 0.18;
    end
end
%
 %% Calculations %%

% entry and exit angle %

h_buildup = (h0*(cotd(Xc))/(cotd(phi))/100)          ;  % snow build up
h_buildup_2 = slipY.*(h0*(cotd(Xc))/(cotd(phi))/100);  % snow build up
h0 = h0/100                                          ;  % penertration depth (convert from cm to m)
theta_f = acosd(1-(h0+h_buildup_2)/z)                ;  % wheel entry angle  (rad)
theta_r = -acosd(1-((lambda*(h0+h_buildup_2))/z))    ;  % wheel exit angle   (rad)

% Bulldozing resistance %


R_b = slipY.*(((cotd(Xc)+ tand(Xc+phi))/(1-tand(alpha)*tan(Xc+phi)))*(h0*c+0.5*rho*h0^2*...
    (((cotd(Xc)-tand(alpha))+(((cotd(Xc))-tand(alpha))^2./(tand(alpha)+(cotd(phi))))))))).*9.81 ; % Bulldozing re


% Bulldozing Side force %

Fbull = zeros(size(1,100))';
for i =1:length(slipY)
fbull = @(x) R_b(i,:).*((z - (z.*(cosd(x)))))        ; % Reaction force due to bulldozing phenomenon
Fbull(i,:) = double(integral(fbull,theta_r(i,:),theta_f(i,:)));
end

Fbull_final = Fbull/Fz                               ; % normalized bulldozing force (-)

%% Digging Force %%

%% switch %%
```

```
snow = 1; % 1.D0
          % 2. D1
          % 3. D3
          % 4. D7
          % 5. D14

%% data %%

a=0.16/2 *(100)                  ; % half the contact patch length (m to cm)
z =  0.643/2                     ; % wheel radius (m)
b =  0.175*(100)                 ; % width of the wheel (m)
lambda = 1                       ; % wheel sinkage ratio
rho = 480                        ; % Snow density (kg/m^3)(dependent on snow)...
                                   %(D0 - 480; D1 - 520; D3 - 490; D7 - 510; D14 - 520) )
alpha = 5;                       ; % "camber angle" of claw shaped tread block (deg)
slipX= (linspace(0,1,100))'      ; % slip angle (deg)
h0 = 0.15                        ; % penetration depth of claw shaped tread block (cm)

%% snow density, cohesion stress, friction angle %%

if snow == 1 % D0
    rho = 0.391e3;                      % density (kg/m3)
    c = 438.33                          ;% cohesion stress of the snow (kgf/m2)
    phi = atand(0.418)                  ;% internal friction angle of snow  (deg) (from Terramechanics)
    Xc = 45 - phi/2                     ;% Destructive angle (deg)
elseif snow == 2 % D1
    rho = 0.406e3;
    c = 621.814
    phi = 12.077                        ;% internal friction angle of snow  (deg)
    Xc = 45 - phi/2                     ;% Destructive angle (deg)
elseif snow == 3 % D3
    rho = 0.397e3;
    c = 897.049
    phi = 13.768                         ;% internal friction angle of snow  (deg)
    Xc = 45 - phi/2                  ;% Destructive angle (deg)
elseif snow == 4 % D7
    rho = 0.398e3;
    c = 1763.507
    phi = 19.188                         ;% internal friction angle of snow  (deg)
    Xc = 45 - phi/2                  ;% Destructive angle (deg)
else snow == 5 % D14
    rho = 0.398e3;
    c = 1386.34
    phi = 12.519                         ;% internal friction angle of snow  (deg)
    Xc = 45 - phi/2                  ;% Destructive angle (deg)
end


%
 %% Calculations %%

% entry and exit angle %
h_buildup = (h0*(cotd(Xc)-tand(alpha))/(tand(alpha)+cotd(phi))/100);  % snow build up (cm to m)
h0 = h0/100;                                          % penertration depth (convertion to m)
% h0 = r*(cosd(theta)-cosd(theta_s))    ;            % 0.01   % wheel sinkage (m) (penetration depth)
theta_f = acosd(1-(h0)/z)              ;            % wheel entry angle  (rad)
theta_r = -acosd(1-((lambda*(h0))/z))    ;          % wheel exit angle   (rad)

% Bulldozing resistance %


R_b = slipX.*(((cotd(Xc)+ tand(Xc+phi))/(1-tand(alpha)*tan(Xc+phi)))*(h0*c+0.5*rho*h0^2*...
    (((cotd(Xc)-tand(alpha))+(((cotd(Xc))-tand(alpha))^2./(tand(alpha)+(cotd(phi))))))).*9.81 ; % Bulldozing re

% Bulldozing Side force %
Fs = zeros(size(1,100))';
for i =1:length(slipX)
fs = @(x) R_b(i,:).*((z - (z.*(cosd(x))))); % Reaction force due to bulldozing phenomenon
Fs(i,:) = double(integral(fs,0,b));% integration consideration full sliding region
Fs_dig = @(x) Fs(i,:);
Fs_dif_final_1(i,:)= double(integral(Fs_dig,0,8,'ArrayValued',true));
```

```
end

%% deflection of brsitle (digging force) %%

w=linspace(0,25.9201,100)';          % 30 kmph to angular speed
w_1 = linspace(0,103.6807,100)';     % 120 kmph to angular speed
slipX_1= (linspace(0,1,100))';
vx = linspace(0,25.9201,100)'.*(0.653/2);           % linear speed 30kmph
vx_1 = linspace(0,103.6807,100)'.*(0.653/2);       % linear speed 120kmph

delta_max = (mu_r2s*Fz)/Cx_r;

chk = vx - w
% xc
z = w.*0.643/2;                      % angular speed carcass (rad/s)
fs = @(x) z;
Fs = double(integral(fs,0,t_bristle,'ArrayValued',true));

% xc
z_1 = w_1.*0.643/2;                  % angular speed carcass (rad/s)
fs_1 = @(x) z_1;
Fs_1 = double(integral(fs_1,0,t_bristle,'ArrayValued',true));

xci = 0 - Fs;                        % from paper
xci_1 = 0 - Fs_1;

% xr
zx = vx;                             % angular speed bristle bottom (rad/s)
fsx = @(x) zx;
Fsx = double(integral(fsx,0,t_bristle,'ArrayValued',true));

xri = 0 - Fsx;                       % from paper

% xr
zx_1 = vx_1;                         % angular speed bristle bottom (rad/s)
fsx_1 = @(x) zx_1;
Fsx_1 = double(integral(fsx_1,0,t_bristle,'ArrayValued',true));

xri_1 = 0 - Fsx_1;                   % from paper

delta_vary_2 = Cx_r.*(xci - xri);        % varying speed (30kmph)
delta_vary_3 = Cx_r.*(xci_1 - xri_1);    % varying speed (120kmph)

delta_vary_2 = delta_vary_2 .*(delta_vary_2<delta_max)
delta_vary_3 = delta_vary_3 .*(delta_vary_3<delta_max)

digdig_2 = @(x) delta_vary_2;
DIGG_2_vary = double(integral(digdig_2,0,.03,'ArrayValued',true));% length on contact patch

digdig_3 = @(x) delta_vary_3;
DIGG_3_vary = double(integral(digdig_3,0,.03,'ArrayValued',true));% length on contact patch


%% Combination of forces %

Fx_r2s = ((Fax_r + Fsx_r).*(slipX<slipX_lim_r)  + (slipX>slipX_lim_r)*mu_r2s*Fz);
Fx_s2s = ((Fax_s + Fsx_s).*(slipX_s<slipX_lim_s) + (slipX_s>slipX_lim_s)*mu_s2s*Fz);

Fy_r2s = ((Fay_r + Fsy_r).*(slipY<slipY_lim_r).*(slipY>-slipY_lim_r) + (slipY>slipY_lim_r)*mu_r2s*Fz -(slipY<-sl
Fy_s2s = ((Fay_s + Fsy_s).*(slipY<slipY_lim_s).*(slipY>-slipY_lim_s) + (slipY>slipY_lim_s)*mu_s2s*Fz -(slipY<-sl

Fx_s2s_1 = zeros(zero_length,1);
Fx_s2s = Fx_s2s;
Fx_s2s_2 = zeros(zero_length,1);

Fx_s2s = vertcat(Fx_s2s_1,Fx_s2s);

Fx_winter = Fx_r2s + Fx_s2s;
Fy_winter = Fy_r2s + Fy_s2s;
```

```
load('digging_D7');% digging in contact patch (choose snow)
Fd = Fs_dif_final_1/4000; % normalized braking force due to digging

load('snow_braking_force.mat');% snow braking force
F_br = void_case_4(3,4); % choose void_case_x(load,type of snow)

load('bulldozing.mat');
load('bulldozing_D7_25mm'); % type of snow and depth
                            % load from bulldozing_V2 script depending on case (lateral)



Fx_util_brk = (Fx_winter/Fz) + (F_br/(Fz*1000)) + Fd; % braking wheel
Fx_util_acc = (Fx_winter/Fz) - (F_br/(Fz*1000)) + Fd + Fd_acc.*(slipX>slipX_lim_r); % traction wheel
Fx_util = (Fx_winter/Fz);   % only snow shear
Fy_util = (Fy_winter/Fz);   % without bulldozing resistance

Fy_util_BB = Fy_winter/Fz + Fbull_final + Fd.*(slipX>slipX_lim_r); % with bulldozing resistance
% bulldozing is normalized

%% end %%
```

Bibliography

[1] Y. Nakajima, "Analytical model of longitudinal tire traction in snow," *Journal of Terramechanics*, vol. 40, pp. 63-82, January 2003.

[2] A. Kusachov, F. Bruzelius, M. Hjort and B. Jacobson, "A double interaction brush model for snow conditions," *Tire Science and Technology*, 2018.

[3] G. Ishigami, "Terramechanics-based Analysis and Control for Lunar/Planetary Exploration Robots," *Doctor of Philosophy Dissertation*, Department of Aeropsace Engineering, Tohoku University, March 2008.

[4] T. Muro and R. N. Yong, "Rectangular plate Loading test on snow - Mobility of tracked oversnow vehicle," *Journal of the Japanese Society of Snow and Ice*, vol. 42, no. 1, pp. 17-24, February 1980.

[5] T. Muro and R. N. Yong, "Vane cone test of snow - Mobility of tracked oversnow vehicle," *Journal of the Japanese Society of Snow and Ice*, vol. 42, no. 1, pp. 25-32, February 1980.

[6] A. L. Browne, "Tire Traction on Snow-Covered Pavements," *The Physics of Tire Traction: Theory and Experiment*, General Motors Research Laboratories, Michigan, Springer Science, pp. 99-139, 1974.

[7] W. R. Janowski, "Tire Traction Testing in the Winter Environment," *SAE Passenger Car Meeting and Exposition, Dearborn*, Technical Paper 800839, June 1980.

[8] T. Muro and J. O'Brien, "Terramechanics: Land Locomotion Mechanics," A. A. Balkema, pp. 19-29, 2004.

[9] S. Kinoshita, "Compression of Snow at constant speed," *International Conference on Physics of Snow and Ice*, The Institute of Low Temperature Science, Hokkaido University, Japan, vol. 1, no. 1, pp. 911-927, 1967.

[10] M. Hjort, O. Eriksson and F. Bruzelius, "Comprehensive Study of the Performance of Winter Tires on Ice, Snow, and Asphalt Roads: The Influence of Tire Type and Wear," *Tire Science and Technology*, TSTCA, vol. 45, no. 3, pp. 175-199, July-September 2017.

[11] S. Ludvigsen, "Improving Mechanical Grip on Winter Tires," *Master's Thesis in Technology and Safety in the High North*, UiT - The arctic University of Norway, June 2017.

[12] S. W. Brown, W. G. M. Vanlaar and R. D. Robertson, "Winter Tires: A Review of Research on Effectiveness and Use," *Traffic Injury Research Foundation, Ottawa*, February 2012.

[13] J. Svendenius, "Tire Models for use in Braking Applications," *Licentiate Thesis*, Department of Automatic Control, Lund Institute of Technology, November 2003.

[14] F. Bruzelius, "Lecture 4 – Tire Modelling.", *Tire and Vehicle Dynamics - FTME030*, Chalmers University of Technology, Sweden, February 2018.

[15] F. Bruzelius, M. Hjort and J. Svendenius, "Validation of a basic combined-slip tyre model for use in friction estimation applications," *Journal of Automobile Engineering*, vol. 228, no. 13, pp. 1622-1629, July 2014.

[16] A. Mehta and G. C. Barker, "The dynamics of sand," *Reports on Progress in Physics*, 1994.

[17] G. Ishigami, A. Miwa, K. Nagatani and K. Yoshida, "Terramechanics-Based Model for Steering Maneuver of Planetary Exploration Rovers on Loose Soil," *Journal of Field Robotics*, vol. 24, no. 3, pp. 233-250, February 2007.

[18] Y. Khedkar, T. Dey and Y. Padasalagi, "Study of Forces Acting on Excavator Bucket While Digging," *Journal of Applied Mechanical Engineering*, vol. 6, no. 5, 2017.

[19] S. Ripka, G. Gäbel, and M. Wangenheim, "Dynamics of a Siped Tire Tread Block-Experiment and Simulation," *Tire Science and Technology*, TSTCA, vol. 37, no. 4, pp. 323-339, October-December 2009.

[20] J. Svendenius and B. Wittenmark, "Brush Tire Model With Increased Flexibility," *Department of Regulatory Technology, Lunds Universitet*, 2003.

[21] T. Linke, K. Wiese, M. Wangenheim, B. Wies and J. Wallaschek, "Investigation of Snow Milling Mechanics to Optimize Winter Tire Traction," *Tire Science and Technology*, TSTCA, vol. 45, no. 3, pp. 162-174, July-September 2017.

[22] S. Ella, P-Y. Formagne, V. Koutsos and J. R. Blackford, "Investigation of rubber friction on snow for tyres," *Tribology International*, vol. 59, pp. 292 - 301, March 2013.